Accepted Manuscript

*Quarterly Journal of Engineering Geology and Hydrogeology*

# Enhancing the Visualisation and Analysis of Geotechnical Properties. Examples from the 3D Volume Change Potential of UK Clay Soils

L. D. Jones, R. Terrington & A. Hulbert

DOI: https://doi.org/10.1144/qjegh2023-160

To access the most recent version of this article, please click the DOI URL in the line above. When citing this article please include the above DOI.

Received 18 December 2023
Revised 28 March 2025
Accepted 12 May 2025

# Enhancing the Visualisation and Analysis of Geotechnical Properties. Examples from the 3D Volume Change Potential of UK Clay Soils

**L. D. Jones*, R. Terrington & A. Hulbert**

British Geological Survey, Keyworth, Nottingham. NG12 5GG UK

*Corresponding Author: ldjon@bgs.ac.uk

This paper builds on the work previously presented in *QJEGH 44* by Jones and Terrington (2011) in two ways; firstly, it expands on the scope of the work adding nine more clay soils to that of the previously reported London Clay and secondly, it builds and improves on the use and type of visualisation and analysis undertaken to model them.

***Abstract***

Ground shrinkage due to shrink–swell clay soils is the most damaging geohazard in the UK, costing the economy an estimated £3.4B over the past 10 years. The towns, cities and infrastructure most susceptible to this shrink–swell behaviour are found mainly in the southeast of the country. Ten of these clay-rich soils have been used in this study. The Volume Change Potential (VCP) of a soil is the relative change in volume to be expected with changes in soil moisture content and is reflected by shrinking and swelling of the ground. Variations in plasticity with area and with depth can be depicted using purely statistical methods. To construct a more representative model of spatial VCP variation in clay-rich formations a more sophisticated 3-D interpolation is required, such as lithofacies modelling which can be used to produce multiple realisations of the variation of parameters, such as the lithology, across a domain where there is an abundance of XYZ data from boreholes or point samples. Virtalis GeoVisionary provides a means of viewing the lithofacies type generated data in a fully immersive 3-D environment. Similar visualisation can be carried out against many environmental parameters and geoscience datasets such as borehole, geophysical data, point clouds, CAD models etc. Voxel models are easily imported and are able to be visualised in their 'true' spatial position, overlying geology or standard maps. The Geosure Shrink–Swell 3D dataset, created using Esri ArcGIS, provides a regional susceptibility model of potential shrink–swell hazard in the London and Thames Valley area. 2-D representations based on statistical analyses show general trends; but with large amounts of data unevenly spread over a wide area, the detail is lost. 3-D models, such as those created using voxelated facies techniques, provide a seamless interpolation and deliver a visualization of VCP that can be interpreted across a variety of depths.

***Key Words***

Geotechnical properties; volume change potential; shrink–swell; clay soils; 3D visualisation.

Many towns, cities, transport routes and buildings are founded on clay-rich soils and rocks in the UK. The clays within these materials may be a significant hazard to engineering construction due to their ability to shrink or swell with seasonal changes in moisture content (often related to rainfall and the evapo-transpiration of vegetation), local site changes such as leakage from water supply pipes or drains, changes to surface drainage and landscaping (including paving) or following the planting, removal or severe pruning of trees or hedges.

In the UK, the effects of shrinkage and swelling of clay soils, with respect to foundation and building damage, were first recognised by geotechnical specialists following the dry summer of 1947, and since then the cost of damage due to shrinking and swelling clay soils has risen dramatically. Over the past 10 years the adverse effects of shrink-swell behaviour has cost the economy an estimated £3 billion, making it the most damaging geohazard in Britain today (Jones & Jefferson, 2012). The Association of British Insurers has estimated that the average cost of shrink–swell related subsidence to the insurance industry stands at over £400 million a year (Driscoll & Crilly, 2000), and that by 2050 this could rise to over £600 million.

Engineering Geologists at the British Geological Survey (BGS) have been investigating the geotechnical and mineralogical factors controlling volume change behaviour of UK clay soils and mudrocks for over 20 years. Formations studied include the Gault (Forster et al, 1994 and Jones & Hobbs, 1998a), the Mercia Mudstone Group (Jones & Hobbs, 1998b and Hobbs et al, 2002), the Lambeth Group (Jones, 2001 and Jones & Hobbs, 2004), the Lias Group (Hobbs et al, 2012), the London Clay Formation (Jones & Terrington, 2011) and the Wealden Group (Freeborough et.al., 2011).

In the UK, towns and cities built on clay-rich soils most susceptible to shrink–swell behaviour are found mainly in the south-east of the country, ten of these clay-rich soils have been used in this study (Figure 1). In these areas many of the 'clay' formations are too young to have been changed into stronger 'mudstones', leaving them still able to absorb and lose moisture. Clay rocks elsewhere in the country are older and have been hardened by processes resulting from deep burial and are less able to absorb water. The clay-soils in this paper are both relatively young clays (e.g. London Clay), weak to very-weak mudstones (e.g. Mercia Mudstone) or interbedded mudstones (e.g. Lias). Some areas (e.g., around The Wash and under the Lancashire Plain) are deeply buried beneath other (superficial) soils that are not susceptible to shrink–swell behaviour. However, other superficial deposits such as alluvium, peat and laminated clays can also be susceptible to soil subsidence and heave (e.g., in the Vale of York and the Cheshire Basin). The depth to which shrinkage and swelling occurs is usually confined to the active zone (upper 1.5m) where moisture change and weathering processes are most likely to occur, unless this zone is extended by the presence of tree roots (Driscoll, 1983).

**Figure 1 – Distribution of UK clay-rich soil formations used in this study (alphabetical order).**

In the UK, some Mesozoic and Neogene & palaeogene (Tertiary) clay soils and weak mudrocks, including the London Clay Formation, are susceptible to shrinkage and swelling as environmental conditions change (Harrison et al, 2012). Indications are that climate change will have an increasingly adverse effect on the moisture conditions that UK soils experience and therefore on the damage caused to homes, buildings and roads. The Government has recognised that climate change is one of the biggest problems that the UK faces and, if current predictions are correct, we can expect hotter, drier summers in the south-east of England, including the areas underlain by these clay-rich soils, and milder, wetter winters, in the rest of the UK (UKCP, 2018). The shrink–swell process is controlled by temperature and the amount of rainfall, and their distribution throughout the year. It also depends on the amount of expansive clay minerals in the soil, the more expansive clay minerals, such as smectite, it contains the higher its swell potential and the more water it can absorb. The change in the amount and distribution of rainfall, as a result of climate change, will lead to a significant increase in the damage done by the shrinking and swelling behaviour of these clay soils. In fact, as many as one in five homes in England and Wales are likely to be damaged by ground that swells when it gets wet and shrinks as it dries out (Jones, 2004). If the UK were to experience an increase in extended periods of dry weather, prior to future rainfall events, costs could rise significantly.

### *Formation Information*

The basic geotechnical properties and mineralogy of the major clay-rich formations in the UK are well known, and well documented throughout the published literature. Therefore, it was determined that it would be unnecessary to add to this. However, onshore sub-crop, outcrop and total area coverage of Great Britain (based on the BGS 1:250k digital geology map – DigMap 250k) for the ten formations are given in Table 1, along with some useful references detailing their typical engineering descriptions, geology and mineralogy.

**Table 1 – Formation Information (alphabetical order)**

### *Volume Change Potential*

The Volume Change Potential (VCP) of a soil is the relative change in volume to be expected with changes in soil moisture content and is reflected by shrinking and swelling of the ground. That is, the extent to which the soil shrinks as it dries out, or swells when it gets wet.

The methodology for determining the VCP of the soils in this study was that determined by Jones & Terrington (2011) based on the Modified Plasticity Index (Ip') proposed in the Building Research Establishment Digest 240 (1993). The data was sourced from the BGS National Geotechnical Properties Database. At the time of this study, the national database contained data from more than 95,000 boreholes, comprising nearly 460,000 geotechnical samples, with over 116,000 containing relevant plasticity data. The data validation and statistical evaluation processes were carried out in accordance with the methodology recommended by Jones & Terrington (2011) in order to quantify the Ip' of the soils across their outcrops. After data validation the number of 'acceptable' plasticity values used for the spatial interpretation was 41,575.

To try and quantify the VCP of all ten formations a preliminary statistical evaluation of the $I_P$' values was carried out to determine the overall range of the data values with respect to their locations across the outcrop. This was carried out by plotting $I_P$' values against their Easting and Northing positions (Figures 2a and 2b) to determine if any west-east, or north-south, trends of increasing plasticity were evident (Jones & Terrington, 2011).

**Figures 2a and 2b – Spread of data samples (whole outcrop) in West-East and North-South directions**

Figures 3a and 3b show the linear trend lines generated on the data, without the samples displayed. They show distinct directional trends of increasing plasticity for the formations:

- West-East & South-North: Atherfield Clay (AC), London Clay (LC), Oxford Clay (OXC)
- West-East & North-South: Gault (GLT)

- West-East only: Mercia Mudstone Group (MMG)
- East-West & South-North: Wadhurst Clay (WDC), Weald Clay (WC)
- East-West & North-South: Kimmeridge Clay (KC), Lambeth Group (LMBE), Lias Clay (LIAS)

**Figures 3a and 3b – Trend lines showing West-East and North-South direction.**

Summary statistics for these data across the ten outcrops are presented in Table 2. These include a *count* of the number of Ip' data points for each formation, the *minimum*, *maximum*, *mean, mode* and *median* values and a series of inter-quartile values, including the *upper quartile*, the *lower quartile* values. These statistics are illustrated in the form of extended box and whisker plots (Figure 4). Extended box plots are constructed from the 0.5$^{th}$, 2.5$^{th}$, 10$^{th}$, 25$^{th}$, 50$^{th}$, 75$^{th}$, 90$^{th}$, 97.5$^{th}$ and 99.5$^{th}$ percentiles of the data sets. The selected percentiles have been chosen as a compromise between practical geotechnics and statistical rigour (Hallam, 1990 and Jones & Terrington, 2011).

**Table 2 – Statistical analysis of $I_P$'**

**Figure 4 – Extended Box & Whisker plots of $I_P$' data values, by formation**

Although, statistically, the median (50$^{th}$ percentile) value would normally be used as the most representative of shrink–swell behaviour, it was decided that in order to portray the 'worst-case' scenario, and represent a greater proportion of the data, the procedure determined by Jones & Terrington (2011) utilising the upper quartile (75$^{th}$ percentile) value would be used in this study.

The VCP was calculated from the statistically analysed $I_P$' data and a classification made based on the *upper quartile* values. The $I_P$' values for the 41,575 data points were each allocated a classification ranging from 'Non-Plastic' to 'Very High', these subdivisions are shown in Table 3 and the percentage VCP, by classification, are summarised in Table 4.

**Table 3 – Classification of VCP (Jones & Terrington, 2011; BRE 1993)**

**Table 4 – Range and amount of VCP calculated by formation**

Table 2 shows that the Gault (GLT) and London Clay (LC) both have upper quartile values of $I_P$' of ≥ 50% and the Atherfield Clay (AC) has a value of 48%, giving them all a VCP of *HIGH*. However, Figure 4 and Table 4 show that 71% GLT and 67% LC samples fall in the High to Very High classification range, and 90% AC samples fall in the Medium to High range.

Table 2 shows that the Kimmeridge Clay (KC), the Oxford Clay (OXC) and the Lambeth Group (LMBE) have upper quartile values of $I_P$' of 35 – 40%, giving them all a VCP of *MEDIUM*. However, Figure 4 and Table 4 show that 95% KC and 85% OXC samples fall in the Medium to High classification range, and 95% LMBE samples fall in the Low to High range.

Table 2 shows that the Lias Clay (LIAS) Wadhurst Clay (WDC) and Weald Clay (WC) have upper quartile values of $I_P$' of 30 – 35%, giving them all a VCP of *MEDIUM*. However, Figure

4 and Table 4 show that 76% LIAS and 75% WDC samples fall in the Medium classification range, and 89% WC fall in the Low to Medium range.

Table 2 shows that the Mercia Mudstone Group (MMG) has an upper quartile values of $I_P$' of 17% giving it a VCP of *LOW*. Figure 4 and Table 4 back this up showing that 63% MMG samples fall in the Low classification range.

**Figures 5a, 5b, 5c and 5d – Ip' vs. Depth Profiles (by Formation)**

Plots of Ip' values against depth for the ten formations are presented in Figures 5a (AC, LC, OXC), 5b (GLT, MMG), 5c (WC, WDC) and 5d (KC, LIAS, LMBE). They are grouped in this way because of their similar East-West, North-South trends and to make the data easier to see. These profiles show the sample data based on their depth below ground level.

The profiles in Figures 5a show that, for AC, 90% of the data lie in the Medium to High VCP classification range ($I_P$' = 23 to 58%) with a slight decrease in plasticity with depth. For LC 67% of the data lie in the High to Very High VCP classification range ($I_P$' = 44 to 70%) with a trend of increasing plasticity with depth. For OXC 85% of the data lie in the Medium to High VCP classification range ($I_P$' = 23 to 58%) with a slight decrease in plasticity with depth.

The profiles in Figures 5b show that, for GLT, 71% of the data lie in the High to Very High VCP classification range ($I_P$' = 44 to 74%) with a minimal change in plasticity with depth. For MMG 63% of the data lie in the Low VCP classification range ($I_P$' = 10 to 17%) with a slight increase in plasticity with depth.

The profiles in Figures 5c show that, for WC, 89% of the data lie in the Low to Medium VCP classification range ($I_P$' = 13 to 33%) with a minimal change in plasticity with depth. For WDC 75% of the data lie in the Medium VCP classification range ($I_P$' = 22 to 34%) with a slight decrease in plasticity with depth.

The profiles in Figures 5d show that, for KC, 95% of the data lie in the Medium to High VCP classification range ($I_P$' = 24 to 39% with a slight decrease in plasticity with depth. For LIAS 76% of the data lie in the Medium VCP classification range ($I_P$' = 22 to 33%) with a minimal change in plasticity with depth. For LMBE 95% of the data lie in the Low to High VCP classification range ($I_P$' = 14 to 54%) with a slight decrease in plasticity with depth.

However, with large amounts of data, covering such wide areas, it is difficult to determine the changes in plasticity to any great detail. Therefore, another method of examining the data, such as 3-D modelling, is required.

***Spatial Interpretation***

As shown above, variations in plasticity with area and with depth can be depicted using purely statistical methods. However, the profiles show that these methods do not reveal the true multi-dimensional variation of the formation. To do this a more suitable method of modelling the data, such as 3-D interpolation, is required.

Interpolation estimates values at unknown locations based on known samples (Lam, 1983). The Inverse Distance Weighting (IDW) interpolative technique described by Jones & Terrington (2011) was applied to the data for all 10 formations in order to determine whether any spatial trend in plasticity was evident. IDW (in this instance) is the estimation of The VCP value at any given location determined by a weighted mean of the nearby values. This output value is limited to the range of the values being used to interpolate it, and therefore the average can never be higher than the greatest value, or less than the lowest value.The IDW technique was applied to the dataset using the geostatistical analysis extension in Esri ArcMap 10 Geographical Information system (GIS).

**Figure 6 - IDW interpolation for all formations using mean IP' at each sample location**

To identify whether any directional trend existed in the $I_P$' values for all ten formations, the outcrop were analysed, observing all available sample points, and ignoring variations with depth. However sizable gaps in the distribution of samples across the outcrop were likely to influence the interpolation model. The resulting spatial analysis using the IDW interpolative technique showed that, although there are localised exceptions, possibly a result of the 'bulls-eye' effect, the VCP tends to increase in a West-East direction (Figure 6), with no South-North trend. However, Figure 3a shows that only AC, LC, OXC, GLT and MMG have a West-East trend and Figure 3b shows a definite South-North trend for AC, LC, OXC, WDC and WC.

Jones & Terrington (2011) discuss the issues of generating plots based on geographically sparse data at different depth intervals, down a borehole. They conclude that both sparsity of data and depth have an effect on the interpolation carried out. To generate a statistically defined model, an area with a large amount of well-spaced data, within a specified and statistically influential distance from known sample locations and at variable depth is required. 'Splitting' the data out to its component formations was also deemed necessary.

### *3-D Modelling*

To construct a more representative model of spatial VCP variations in clay-rich formations utilisation of a more sophisticated 3-D modelling and visualisation package is necessary. The NextMap Digital Terrain Model (Intermap Technologies) was used to constrain the data at the ground surface including the boreholes and as the top constraining surface for the voxel models. The original data is 5 m cell resolution. The data was subsampled to a lower resolution (100 m) to ensure the entire dataset could be modelled in the area of interest. The borehole and surface sample information were then 'hung' from the DTM to give it an accurate position below ground level. To visualise the data as accurately as possible, it was decided to create an S-Grid model; a flexible 3-D grid that can be eroded between two boundary horizons to model a volume, e.g. the ground surface (DTM) and the base of the London Clay. Culshaw (2005) gave an example of this approach using SPT 'N' Value data for glacial till in the Manchester/Salford (UK) area. This paper follows the approach used by Jones & Terrington (2011) to create their 3-D VCP model. S-Grid models can also contain multiple property information, and fit the boundaries of the data more accurately.

S-Grid models were created using the '3D grid reservoir builder' in GoCAD™ with the DTM set as the upper limit, the DTM -30m surface as the basal limit and the outcrop of each formation as the area boundary. The modified $I_P$' values were draped onto the S-Grid to 'paint' the grid cells (each cell containing an $I_P$' value was transformed to that $I_P$' value). The grid was then initialised to the *mean* value (derived by the builder), giving all cells without a 'painted' $I_P$' value the *mean value*. The modified $I_P$' values were then interpolated and smoothed throughout the grid, giving a full 3-D image. S-Grids provide a seamless interpolation of the modified IP' data, showing a visualisation that allows the IP' values to be examined relative to ground level, as opposed to just seeing the trends within the data itself. Visualising the data with the DTM gives a greater sense of reality and perspective. Inverse Distance Weighting (IDW) allows only snapshots at different depth intervals but the S-Grid allows interactive and dynamic visualisations of the data at various depths and locations. Combining these GIS and

3-D modelling capabilities, prediction of plasticity and, hence, volume change potential, becomes a realistic prospect.

Looking at the central and eastern area of the London Clay (from Jones & Terrington, 2011) the IDW model shows little variation in plasticity in the uppermost part of the London Clay, which falls mainly within the High VCP class (Figure 7a). However, as the depth increases to 8m plus, an area of increased plasticity equating to a Very High VCP classification, can be seen in the east of the area (Figure 7b). At around 20m depth the VCP in the east remains Very High decreasing to Medium VCP in the west (Figure 7c). This trend continues to a depth of approximately 30m (Figure 7d).

**Figure 7 - S-Grid interpolations for London Clay, showing surfaces at 0m, 8m, 20m and 30m (blue-medium, green-high, yellow/red-very high VCP)**

Facies modelling techniques have been widely used at the BGS to convey lithological variation and heterogeneity of geotechnical parameters (Kearsey et al., 2015 and Kearsey et al., 2011, Woods et. al., 2015) and are a standard geological modelling output for other modern geological surveys, such as the Netherlands Organisation for Applied Scientific Research (TNO) (Stafleu et al., 2012). Facies models can be used to produce multiple realisations of the variation of parameters such as the lithology (e.g. the proportion and grading of sand, gravel, silt and clay) across a domain where there is an abundance of XYZ data from boreholes or point samples. Instead of a sharp boundary depicting the classification of what becomes a stratigraphical horizon as typically shown in geological maps and deterministic models (Kessler et al., 2009), facies modelling allows these lithologies to grade into each other, which better captures the inter-fingered nature of heterolithic geological deposits and their associated physical properties.

Previous attempts to map and model the VCP of the London Clay in central London (Jones and Terrington, 2011) using basic facies techniques showed that the modified plasticity values ($I_P$') used to generate the VCP score ranged from 1 to 80+ and also varied significantly in their XYZ position. The variation in values and the clustered and sometimes linear alignment of the data (coming from road or railway developments) can obscure the visualisation of relationships between the data. Often the XY scale was set at 100 x 100 m, or coarser, but the Z scale tended to be 1 to 2m as the sampling rate downhole is sub-metre. Therefore, the more traditional facies techniques for modelling this type of continuous data, such as IDW, are limited in areas where there are large gaps between the data points and the data is clustered, as $I_P$' values are interpolated beyond what is reasonably expected masking the accuracy and uncertainty in areas where there are few data points.

To gain a better understanding of the variation within the dataset, the $I_P$' values were grouped into the classifications outlined in Table 3. This data was used discretely to produce facies models based on the classifications. The methodology used follows that by Jones et. al. (2017) in SKUA-GOCAD®. The detail and benefits of this methodology are described by Kearsey et al (2015), although there are some fundamental differences between that methodology and the one used in this study; the main one being that physical geotechnical parameters were assessed here; namely $I_P$' and VCP, rather than only the lithological variation assessed in Kearsey et al (2015).

The models created using this technique should show a better reflection of the true nature of the ground conditions relating to the VCP of the clay units. However, these models do not generate good site-specific results and do not capture locally constrained variation, but rather give an overall impression of the shrink–swell properties of that specific clay unit. More detailed site-scale models can be produced for areas where large numbers of boreholes and sample data are situated and evenly distributed.

S-Grid models were created for each of the clipped formation areas and then cross-sections were extracted in order to show the full 3D potential of the technique used. Figure 8 shows the extent of the clipped area of the London Clay, and the VCP values visible at the surface of the formation. The model shows little variation in plasticity across this area, in the surface of the London Clay, falling mostly within the High VCP class, as it showed with the previously discussed IDW model and the simpler S-Grid model.

**Figure 8 - S-Grid model of clipped area of London Clay, showing top surface**

Figure 9 shows the base of the London Clay for the extent of the clipped area, with the $I_P$' sample points displayed with their VCP value, and the lines of the four digitised cross-sections marked. The sections were chosen because they represent areas with large amounts of well-spaced data, usually aligned to a linear feature (such as a road). Digitised cross-section number 1 (Figure 10) confirms the West-East trend of increasing plasticity, whilst also showing that the London Clay, in this area, maintains a High VCP value throughout its depth. S-grid models and cross-sections were also created for the Atherfield Clay, Gault, Lias Clay, Lambeth Group and Mercia Mudstone Group, discussed below. S-grid models were not created for the Kimmeridge Clay, Wadhurst Clay and Weald Clay Formation because the data was too sparsely distributed and the interpolation was not deemed good enough.

**Figure 9 - S-Grid model of clipped area of London Clay, showing areas of digitised cross-sections**

**Figure 1 Digitised cross-section 1 of London Clay, showing VCP values**

Figures 11 to 15 show a single digitised cross-section from each of the other five clipped formation areas, these being Atherfield Clay, Gault, Lias Clay, Lambeth Group, Mercia Mudstone Group. Interpretations of these figures indicate that the Atherfield Clay (Figure 11) shows a slight increase in plasticity in a West-East direction, comparing well with Figure 3a, and an increase with depth in the east. The shape of the lower boundary is disconformable on the Wealden Group throughout the Wessex Basin, on the Vectis Formation in the Vectian Basin, and on the Weald Clay Formation in the Wealden Basin. The Gault (Figure 12) also shows a West-East trend of increasing plasticity. This compares well with the results obtained from Figure 3a, that shows the same West-East trend of increasing plasticity. It also shows that the Gault increases in plasticity with depth, across the section.

**Figure 2 Digitised cross-section 1 of Atherfield Clay, showing VCP values**

**Figure 3 Digitised cross-section 1 of Gault, showing VCP values**

The cross-section of Lias Clay (Figure 13) shows that it maintains a Medium VCP across the section, with no discernible East-West, North-South or depth trend. This compares well with Figure 3a which showed only minor trends. The Lambeth Group (Figure 14) also maintains a

Medium VCP across the section. This does not compare well with the results from Figure 3a which showed slight East-West and North-South trends of increasing plasticity. However, this could be due to the orientation of the sections chosen, or perhaps the lack of data in XY or at depth.

**Figure 4 - Digitised cross-section 1 of Lias Clay, showing VCP values**

**Figure 5 - Digitised cross-section 1 of Lambeth Group, showing VCP values**

Figure 15 shows a West-East cross-section of the Mercia Mudstone Group and confirms the results from Figure 3a that there is no discernible trend in increasing plasticity in either an East-West or North-South direction. The section shows that it maintains a Low VCP throughout, including throughout its depth.

**Figure 6 - Digitised cross-section 1 of Mercia Mudstone Group, showing VCP values**

GeoVisionary is the result of a lengthy collaboration between the BGS and Virtalis Ltd. It is a unique 3D stereographic software system that allows the high-resolution visualisation and interpretation of geospatial data, used for mapping and data interrogation, from continent to site specific scales (Terrington et al, 2015). GeoVisionary also allows the integration of 3D and 4D data, such as 3D geological model data including boreholes (both vertical and deviated), cross-sections and surfaces as well as parameterized voxel models, LiDAR point cloud scans, CAD models of buildings and infrastructure, and time series data that could show land level change or water table variation, for example.

The clipped area of the London Clay formation was re-cropped to form a smaller area (Figure 16) centred around Islington, where there was a large data density of $I_P$' values, making it easier to import into GeoVisionary as a voxel model. The model can be displayed with other geospatial data e.g. the outcrop and underlying geology (Figure 17), or it can be clipped to show a plane of VCP through any section of the model (Figure 18). GeoVisionary can also show either multiple or singular values of VCP; Figure 19, for instance, shows the re-cropped area displaying only the Very High VCP values.

**Figure 7 - GeoVisionary image of S-Grid model of re-cropped area of London Clay, showing VCP values overlaid on Map**

**Figure 8 - GeoVisionary image of S-Grid model of re-cropped area of London Clay, showing outcrop and underlying geology**

**Figure 9 - GeoVisionary image of S-Grid model of re-cropped area of London Clay, showing VCP values as a clipping plane**

**Figure 19 - GeoVisionary image of S-Grid model of re-cropped area of London Clay, showing Very High VCP values**

The BGS GeoSure dataset comprises six different Geographical Information System (GIS) 1:50,000-scale layers, with each layer representing a different natural ground stability hazard that occurs in Great Britain (Walsby, 2008): (1) collapsible ground, (2) running sands, (3) compressible ground, (4) landslides, (5) soluble rocks, and (6) shrink–swell (Figure 20). The current version of the GeoSure data set is v. 9.0 and this was released in 2024. The GeoSure datasets are 2-D polygon (area) layers, resulting from deterministic assessments of appropriate causative factors. Each ground stability geohazard is classified using the same straightforward classification, ranging from 'A' (low hazard potential) to 'E' (high hazard potential). The GeoSure shrink–swell layer was used to determine the VCP values for the clay soils herein. Figure 20 shows the shrinkage potential of all the lithologies across the UK mainland as moderate or significant. This potential can be shown at greater resolution but is lost on such a small scale map.

The GeoSure shrink–swell 3D dataset, produced in 2023, is an addition to the GeoSure ground stability data consists of a single data layer, in GIS format, that identifies areas of potential shrink–swell hazard, in three dimensional space, at intervals down to 20 m in the London Lithoframe* (Mathers et al., 2014) area of Great Britain.

*See http://www.bgs.ac.uk/services/3Dgeology/lithoframe.html.

**Figure 20 - UK map of GeoSure shrink–swell geohazard. (Lee & Diaz, 2017)**

https://www.bgs.ac.uk/products/geoSure/geoSureLondon.html



The BGS London Lithoframe geological model (Mathers et al., 2014) covers an area extending 120 km east-west and 40 km north-south (4,800 $km^2$). The model was constructed as twelve 20 km x 20 km squares, arranged as six columns in the east-west direction and two rows in the north-south direction (Figure 21). The GeoSure Shrink–Swell 3D model uses the twelve subareas defined by the London Lithoframe model, and within them it contains the shrink-swell characteristics of the top 20m of the London Clay.

**Figure 10 - Coverage of the Shrink–Swell 3D dataset.**



Esri ArcGIS was used to create the GeoSure Shrink–Swell 3D model. The model area was defined by a regular 50 m x 50 m grid; then converted to a point feature class, with each point located at the center of a grid cell. The Nextmap DTM (Intermap Technologies, 2007) defined the ground elevation (related to Ordnance Datum) of each point. A custom Python script assessed the presence below each point of geological formations at nine specific depths (at 0 m, 1 m, 2 m, 3 m, 4 m, 5 m, 6 m, 7 m, 8 m, 9 m, 10 m, 15 m and 20 m), and stored this information as an attribute-string attached to each point. A second custom python script converted this attributed point dataset to a series of nine gridded surfaces with 50 m x 50 m resolution, each defining the geological conditions at the specified depth.

The GeoSure Shrink–Swell 3D product was created by "stacking" these gridded surfaces to produce a dataset that defined, for each 50 m cell, the geological conditions at the nine specified depths. It was then a straightforward process to convert this dataset into one that had attributes defining 3-D VCP values at specified depth intervals within this upper 20 m across the entire BGS London Lithoframe model. To ensure the compatibility of the GeoSure Shrink–Swell 3D product with the existing standard 2-D GeoSure Shrink–Swell product, two additional attributes were added for each 50 m cell, the dominant (modal) VCP value and the range of the VCP values. The GeoSure Shrink–Swell 3D product provides GIS gridded maps for each of the twelve 20 km x 20 km squares; these display the VCP values at any of the specified depths (Figure 22). Alternatively, a tabulation of the vertical distribution of VCP values for each 50 m x 50 m cell can be requested (Table 5).

**Figure 22 - Distribution of Volume Change Potential (VCP) values at specified depths below ground within a 20 km x 20 km square (yellow-low, blue-medium, green-high, red-very high)**

**Table 1 - Example of GeoSure Shrink–Swell 3D tabulation for a 50 m x 50 m cell**

**Key:**

MGR Made Ground ALV Alluvium LASI Langley Silt LC London Clay

## *Conclusions*

- 2-D representations, based on statistical analyses, of the VCP in the London Clay show general trends. 3-D models, such as those created by the S-Grid and facies techniques, provide a seamless interpolation and deliver a visualization of VCP that can be interpreted across a variety of depths.
- The calculated upper quartile (75$^{th}$ percentile) value of Modified Plasticity Index ($I_P$') across the entire onshore outcrop of London Clay (LC), Gault (GLT) and Atherfield Clay (AC) is indicative of a High Volume Change Potential (VCP).
- The calculated upper quartile (75$^{th}$ percentile) value of Modified Plasticity Index ($I_P$') across the entire onshore outcrop of Lambeth Group (LMBE), Lias Clay (LIAS), Weald Clay (WC), Oxford Clay (OXC), Kimmeridge Clay (KC) and Wadhurst Clay (WDC) is indicative of a Medium Volume Change Potential (VCP).
- The calculated upper quartile (75$^{th}$ percentile) value of Modified Plasticity Index ($I_P$') across the entire onshore outcrop of Mercia Mudstone Group (MMG) is indicative of a Low Volume Change Potential (VCP).
- Both the statistical and spatial analyses confirm a West-East and a South-North trend of increasing plasticity and, hence, VCP for Atherfield Clay (AC), London Clay (LC) and Oxford Clay (OXC).
- Both the statistical and spatial analyses confirm a West-East and a North-South trend of increasing plasticity and, hence, VCP for Gault (GLT). They also show a increase in plasticity with depth.
- Both the statistical and spatial analyses confirm a West-East only trend of increasing plasticity and, hence, VCP for Mercia Mudstone Group (MMG).
- Both the statistical and spatial analyses confirm an East-West and a South-North trend of increasing plasticity and, hence, VCP for Wadhurst Clay (WDC) and Weald Clay (WC).
- Both the statistical and spatial analyses confirm no trend of increasing (or decreasing) plasticity and, hence, VCP in any direction for Kimmeridge Clay (KC), Lias Clay (LIAS).
- The statistical analysis confirms a slight East-West trend of increasing plasticity and, hence, VCP for Lambeth Group (LMBE), but the spatial analysis showed no sign of this trend.

- 2-D representations based on statistical analyses show general trends of increasing and/or decreasing VCP; but with large amounts of data unevenly spread over a wide area, the detail is lost.
- The **Inverse Distance Weighting** (**IDW**) spatial modelling technique is affected by the data distribution, calling into question the validity of the predicted model. In effect the output value can never be higher than the greatest value, or less than the lowest value, whereas 3-D models, such as those calculated by **S-Grid**, provide a seamless interpolation, giving a visualisation that allows the $I_P$' values to be examined at a variety of depths relative to ground level.
- London Clay (LC): The results of the modelling have confirmed variations of VCP with depth across central and east London and south Essex as follows:
    - Near-surface – Little variation, the VCP is High across the area.
    - 8-20 m – Increasing plasticity east of London, around the mouth of the Thames, VCP changes from High to Very High.
    - 20-30 m – Decrease in plasticity in central London (Area 3a), VCP changes from High to Medium. Plasticity remains the same in the east, VCP is Very High.
    - >30 m* – Decrease in plasticity in east, VCP changes from Very High to High. Plasticity remains the same in central London, VCP is Medium (***not shown**).
- **Lithofacies (Facies) Modelling** using S-Grids allows for a more realistic representation of this type of physical properties data ($I_P$', VCP, BD, DD, PSA etc.). It allows attributes to grade into each other, which better captures their inter-fingered nature and the variability of the subsurface.
- The main aim of the facies modelling were to show that VCP values can be used as a proxy to show the variability of shrinking and swelling clays particularly along linear alignments, which is how much of the data was spatially distributed.
- Further study would prove useful in determining how good these types of models are at demonstrating the 'true' nature of these types of physical properties data along linear alignments. The potential of this work could save time and money for relevant businesses, especially those related to underground services and infrastructure, and where climate change influences these (Rotta Loria, 2023).
- Further work could be undertaken in order to include bootstrapping techniques whereby proportions of the data are removed from the conditioning data and then the simulation is re-run without that data and the results compared. This process would be repeated a number of times, allowing the user to quantify the reliability of predictions in the facies model.
- **Geovisionary** provides a means of viewing the facies type generated data in a fully immersive 3-D, or even 4-D, environment. This type of environment lends itself to both education and research as well as to visualisation and modelling. Voxel models are easily imported and are able to be visualised in their 'true' spatial position, overlying geology or standard maps. The data values can be shown as sections using clipping planes in any direction, or specific data values can be extracted to show where these occur spatially in order to predict possible tendencies, or show actual trends in the data.

It can be used in tandem with many other datasets to provide insights you would not necessarily get from looking at the data in isolation in a modelling package.

- The **GeoSure Shrink–Swell 3D** model for London is part of the BGS GeoSure range of natural subsidence products. Based on data contained within the London Geological Model (Mathers et al., 2014) it provides a regional susceptibility model of potential shrink–swell hazard, in 3-D, at intervals down to 20 m in the London and Thames Valley area.
- The Geosure Shrink–Swell 3D dataset provides an information resource for asset and infrastructure development and maintenance. The shrink-swell properties of the London Clay affect developers, construction companies, and local government due to increased costs of insurance, additional engineering works to stabilize land, or potential relocation of developments. Information on the 3-D distribution of shrink-swell properties permits identification of potential problems at the surface, in the shallow sub-surface, or deeper underground.
- This type of modelling could be used for many applications in the construction industry, especially those relating to infrastructure development and maintenance., These type of scenarios would lend themselves well to applications such as climate change and temperature anomalies, in the ground beneath London (for example), and the thermal imprint of heat islands, due to underground transport (inc. trains braking), residential basement and paving of previously open spaces (Bidarmaghz et al., 2020).

*Acknowledgements*

This paper is published with the permission of the Executive Director of the British Geological Survey.

**Author contributions**

All authors have read and agreed to the published version of the manuscript.

**Funding information**

This research received no external funding.

**Data availability statement**

BGS data is available at www.bgs.ac.uk.

*References*

Bidarmaghz, A., Choudhary, R., Soga, K., Terrington, R., Kessler, H. and Thorpe, S. 2020. Large-scale urban underground hydro-thermal modelling – A case study of the Royal Borough of Kensington and Chelsea, London. Science of the Total Environment, V. 700, 15 January, 2020. https://doi.org/10.1016/j.scitotenv.2019.134955

BRE (1993) Low-rise buildings on shrinkable clay soils: BRE Digest, Vols. 240, 241 & 242. CRC, London.

Building Research Establishment (BRE) 1993. *Low-rise buildings on shrinkable clay soils*: Part 1, Digest 240. Building Research Establishment. Watford

Cox, B.M., Sumbler, M.G. and Ivimey-Cook, H.C. 1999. A Formational framework for the Lower Jurassic of England and Wales (Onshore Area). British Geological Survey Research Report Series No.RR/99/01

Cox, B.M., Hudson, J.D. and Martill, D.M. 1992. Lithostratigraphic nomenclature of the Oxford Clay (Jurassic). Proceedings of the Geologists' Association, **103**, 343-345

Culshaw, M.G. 2005. From concept towards reality: developing the attributed 3D geological model of the shallow subsurface. Quarterly Journal of Engineering Geology and Hydrogeology, **38**(3), 231-284

Driscoll, R. 1983. The influence of vegetation on the swelling and shrinking of clay soils in Britain. *Geotechnikque,* **38**, 93-105

Driscoll R. and Crilly, M. 2000. Subsidence damage to domestic buildings. Lessons learned and questions asked. London: BRE Press

Ellison, R.A., Knox, R.W.O'B., Jolley, D.W. & King, C. 1994. A revision of the lithostratigraphical classification of the early Palaeogene strata of the London Basin and East Anglia. *Proceedings of the Geologists Association*, **105**, 187-197

Forster, A., Hobbs, P.R.N., Cripps, A.C., Entwisle, D.C., Raines, M.G., Hallam, J.R., Jones, L.D., Self, S.J., Meakin, J. 1994. The Engineering Geology of British Rocks and Soils. The Gault Clay in England. British Geological Survey Technical Report Series No. WN/94/31

Freeborough, K., Venus, J. and Kirkham, K. 2011. *Determination of the shrinking and swelling properties of the Weald Clay Formation.* British Geological Survey Internal Report IR/11/035

Hallam, J. R. 1990. *The statistical analysis and summarisation of geotechnical databases*. British Geological Survey, Technical Report WN/90/16

Harrison, A.M., Plim, J., Harrison, M., Jones, L.D. and Culshaw, M.G. 2012. The relationship between shrink–swell occurrence and climate in south-east England. Proceedings of the Geologists' Association, **123**(4), 556-575

Hobbs, P.R.N.; Entwisle, D.C.; Northmore, K.J.; Sumbler, M.G.; Jones, L.D.; Kemp, S.; Self, S.; Barron, M. and Meakin, J.L. 2012. Engineering geology of British rocks and soils : Lias Group. British Geological Survey Open Report Series No. OR/12/032

Hobbs, P.R.N., Hallam, J.R., Forster, A., Entwisle, D.C., Jones, L.D., Cripps, A.C., Northmore, K.J., Self, S.J., Meakin, J.L. 2002. Engineering geology of British rocks and soils: mudstones of the Mercia Mudstone Group. British Geological Survey Research Report Series No.RR/01/002

Hopson, P M, Farrant, A R and Booth, K A. 2001. Lithostratigraphy and regional correlation of the basal Chalk, Upper Greensand, Gault and Uppermost Folkestone formations (Mid-Cretaceous) from cored boreholes near Selborne, Hampshire. Proceedings of the Geologists' Association, **112**, 193-210

Hopson, P.M., Wilkinson, I.P. and Woods, M.A. 2008. *A stratigraphical framework for the Lower Cretaceous of England*. Research Report RR/08/03. British Geological Survey, Keyworth

Horton, A., Sumbler, M.G., Cox, B.M. and Ambrose, K. 1995. Geology of the country around Thame. Memoir of the British Geological Survey, Sheet 237 (England and Wales)

Howard, A.S., Warrington, G., Ambrose, K., and Rees, J.G. 2008. A formational framework for the Mercia Mudstone Group (Triassic) of England and Wales. British Geological Survey Research Report Series No. RR/08/04

Intermap Technologies 2007. NEXTMap British Digital Terrain Model Dataset. Produced by Intermap. NERC Earth Observation Data Centre

Jones, L.D., Terrington, R. and Hulbert, A. 2017. Methods for Modelling the 3D Volume Change Potential of UK Clay Soils. British Geological Survey Research Report RR/17/008

Jones, L.D. and Jefferson, I. 2012. Expansive soils. In: Burland, J., Chapman, T., Skinner, H., Brown, M. (Eds.), ICE manual of geotechnical engineering. Volume 1 Geotechnical engineering principles, problematic soils and site investigation. London: ICE Publishing, 413-441

Jones, L.D. and Terrington R. 2011. Modelling volume change potential in the London Clay. Quarterly Journal of Engineering Geology and Hydrogeology, **44**, 1-15

Jones, L.D. and Hobbs, P.R.N. 2004. The Shrinkage and Swelling Behaviour of UK Soils: Clays of the Lambeth Group. British Geological Survey Research Report Series No. RR/04/01

Jones, L.D. 2001. Determination of the shrinking and swelling properties of the clays of the Lambeth Group. British Geological Survey Internal Report Series No. IR/01/54

Jones, L.D. and Hobbs, P.R.N. 1998a. The Shrinkage and Swelling Behaviour of UK Soils: Gault Clay. British Geological Survey Technical Report Series No. WN/98/13

Jones, L.D. and Hobbs, P.R.N. 1998b. The Shrinkage and Swelling Behaviour of UK Soils: Mercia Mudstone. British Geological Survey Technical Report Series No. WN/98/14

Kearsey, T., Williams, J., Finlayson, A., Williamson, P., Dobbs, M., Marchant, B., Kingdon, A., and Campbell, D. 2015. Testing the application and limitation of stochastic simulations to predict the lithology of glacial and fluvial deposits in Central Glasgow, UK. Engineering Geology, **187**, 98-112

Kearsey, T., Finlayson, A., Williamson, P., Williams, J.D.O., Terrington, R.L., Kingdon, A. and Campbell, S.D.G. 2011. Comparing and fusing deterministic and stochastic geological models: an example from the City of Glasgow, UK. Model Fusion Conference, London, UK, 28-29 Nov 2011 (Unpublished) http://nora.nerc.ac.uk/16001

Kessler, H., Mathers, S. and Sobisch, H-G. 2009. The capture and dissemination of integrated 3D geospatial knowledge at the British Geological Survey using GSI3D software and methodology. *Computers & geosciences*, **35**(6), 1311-1321

King, C. 1981. The stratigraphy of the London Clay and associated deposits. *Tertiary Research Special Papers*, **6**, 1-158

Lam, N.S. 1983. Spatial Interpolation methods: A review. *The American Cartographer*, **10**, 129-149

Lee, K.A. and Diaz Doce, D. 2017. User Guide for the British Geological Survey GeoSure dataset: Version 8. British Geological Survey Report Open Series OR/17/050

Mathers, S.J., Burke, H.F., Terrington, R.L., Thorpe, S., Dearden, R.A., Williamson, J.P. & J.R. Ford 2014. A Geological Model of London and the Thames Valley, Southeast England. Proceedings of the Geologists' Association. **125**, 373-382

Reeves, G.M., Sims, I. & Cripps, J.C. (eds) 2006. *Clay Materials Used in Construction*. Geological Society, London, Engineering Geology Special Publication, 21

Rotta Loria, A. F. 2023. The silent impact of underground climate change on civil infrastructure. Communications Engineering, 44 (2023).

Simpson, M.I. 1985. The stratigraphy of the Atherfield Clay Formation (Lower Aptian, Lower Cretaceous) at the type and other localities in southern England. Proceedings of the Geologists' Association, **96**(1), 23-45

Stafleu, J., Maljers, D., Busschers, F.S., Gunnink, J.L., Schokker, J., Dambrink, R.M., Hummelman, H.J. and Schijf, M.L. 2012. GeoTOP modellering (in Dutch). TNO Report 2012 R10991, 216p

Terrington, R., Napier, B., Buchi, A. and Procopio, P.M. 2015. Managing the mining cycle using GeoVisionary. In: Aachan International 5th Mining Symposia. Aachan, Germany, 27-28 May 2015

United Kingdom Climate Predictions (UKCP) 2018. *Available from:*

https://www.metoffice.gov.uk/research/approach/collaboration/ukcp/index

Walsby, J.C. 2008. GeoSure: A Bridge between Geology and Decision-Makers. IN: Communicating Environmental Geoscience (Liverman, D.G.E., Pereira, C. & B. Marker, eds.). Geological Society, London, Special Publication **305**, 81-87

Woods, M.A., Newell, A.J., Haslam, R., Farrant, A.R. and Smith, H. 2015. A physical property model of the Chalk of Southern England. Nottingham, UK, British Geological Survey Open Report OR/15/013

Table 1

| Formation | On-shore Subcrop | Outcrop | UK Area | References for typical: Engineering Description | References for typical: Geology & Mineralogy |
|---|---|---|---|---|---|
| **Atherfield Clay** | 72 km² | 51 km² | <0.1% | Hopson, Wilkinson and Woods, 2008 | Simpson, 1985 |
| **Gault Clay** | 1441 km² | 785 km² | 0.7% | Forster et al, 1994 | Hopson, Farrant and Booth, 2001 |
| **Kimmeridge Clay** | 2609 km² | 642 km² | 1.2% | Reeves, Sims and Cripps, 2006 | Horton et al, 1995 |
| **Lambeth Group** | 986 km² | 351 km² | 0.5% | Jones and Hobbs, 2004 | Ellison et al, 1994 |
| **Lias Clay** | 8566 km² | 4675 km² | 4.1% | Hobbs et al, 2012 | Cox et al, 1999 |
| **London Clay** | 6493 km² | 2245 km² | 3.1% | Jones and Terrington, 2011 | King, 1981 |
| **Mercia Mudstone Group** | 11999 km² | 3818 km² | 5.7% | Hobbs et al, 2002 | Howard et al, 2008 |
| **Oxford Clay** | 4290 km² | 1324 km² | 2.0% | Reeves, Sims and Cripps, 2006 | Cox et al, 1992 |
| **Wadhurst Clay** | 558 km² | 498 km² | 0.3% | Hopson, Wilkinson and Woods, 2008 | Gallois and Worssam, 1993 |
| **Weald Clay** | 1671 km² | 1342 km² | 0.8% | Hopson, Wilkinson and Woods, 2008 | Gallois and Worssam, 1993 |

| | **LC** | **GLT** | **LMBE** | **MMG** | **LIAS** | **WC** | **OXC** | **KC** | **AC** | **WDC** |
|---|---|---|---|---|---|---|---|---|---|---|
| ***count*** | ***13149*** | ***2724*** | ***4565*** | ***4886*** | ***5929*** | ***1783*** | ***1284*** | ***306*** | ***811*** | ***207*** |
| **min** | 1 | 5 | 1 | 1 | 1 | 2 | 1 | 11 | 2 | 5 |
| **0.005** | 10 | 14 | 2 | 1 | 7 | 6 | 6 | 12 | 7 | 6 |
| **0.025** | 19 | 23 | 7 | 4 | 12 | 9 | 12 | 16 | 14 | 10 |
| **0.1** | 29 | 33 | 14 | 8 | 18 | 13 | 18 | 24 | 23 | 17 |
| **0.25** | 37 | 39 | 20 | 10 | 22 | 19 | 23 | 28 | 30 | 22 |
| **median** | 44 | 44 | 30 | 13 | 27 | 26 | 29 | 33 | 37 | 26 |
| **0.75** | **50** | **51** | **38** | **17** | **33** | **33** | **36** | **39** | **48** | **34** |
| **0.9** | 58 | 62 | 50 | 27 | 43 | 43 | 48 | 47 | 58 | 45 |
| **0.975** | 62 | 67 | 54 | 31 | 47 | 47 | 51 | 48 | 61 | 47 |
| **0.995** | 70 | 74 | 66 | 40 | 56 | 54 | 58 | 56 | 67 | 58 |
| **max** | 84 | 93 | 92 | 57 | 89 | 62 | 69 | 67 | 73 | 62 |
| **mean** | 43 | 45 | 30 | 14 | 28 | 26 | 30 | 33 | 38 | 28 |
| **mode** | 45 | 46 | 30 | 13 | 28 | 29 | 26 | 31 | 30 | 26 |
| **VCP** | **H** | **H** | **M** | **L** | **M** | **M** | **M** | **M** | **H** | **M** |

Table 2

Table 3

| $I_P$' (%) | VCP |
|---|---|
| <10 | Non Plastic |
| 10 - 20 | Low |
| 20 - 40 | Medium |
| 40 - 60 | High |
| >60 | Very High |

| VCP | Percentage of Samples by Classification | | | | | | | | | |
|---|---|---|---|---|---|---|---|---|---|---|
| | LC | GLT | LMBE | MMG | LIAS | WC | OXC | KC | AC | WDC |
| Non-Plastic | - | - | 4 | 19 | 1 | 3 | 1 | - | 1 | 2 |
| Low | 2 | 1 | 18 | 63 | 14 | 25 | 14 | 5 | 5 | 13 |
| Medium | 31 | 28 | 56 | 17 | 76 | 64 | 68 | 73 | 50 | 75 |
| High | 63 | 63 | 21 | 1 | 9 | 8 | 17 | 22 | 40 | 10 |
| Very High | 4 | 8 | 1 | - | - | - | - | 1 | 3 | - |

Table 4

Table 5

| **Depth (mbgl)** | **Formation Code** | **Dominant VCP Ranking** | **Range of VCP Rankings** |
|---|---|---|---|
| 0 | MGR | A | |
| 1 | ALV | C | A-C |
| 2 | ALV | C | A-C |
| 3 | LASI | B | |
| 4 | LASI | B | |
| 5 | LC | D | A-E |
| 10 | LC | D | A-E |
| 15 | LC | D | A-E |
| 20 | LC | D | A-E |

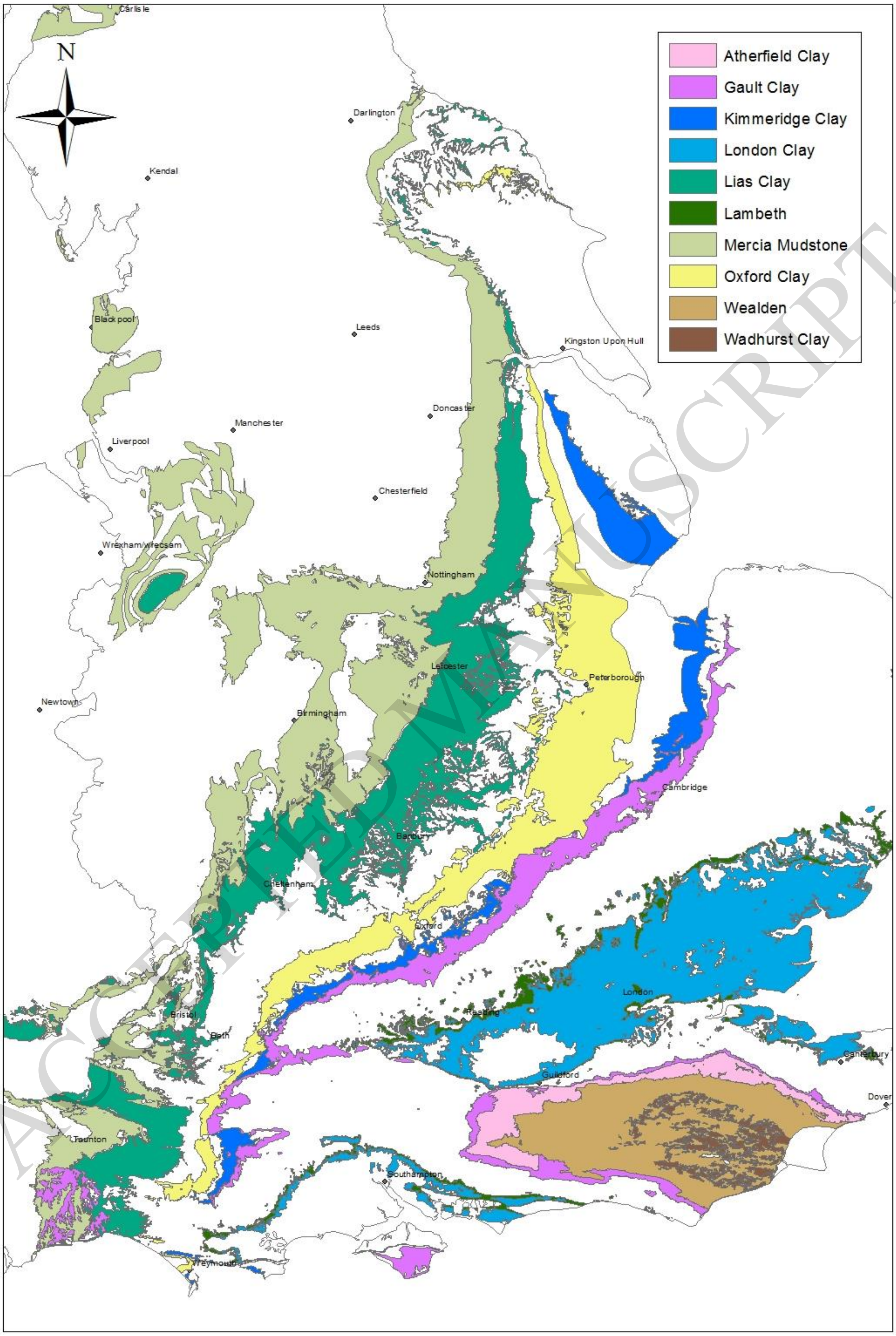
N
Atherfield Clay
Gault Clay
Kimmeridge Clay
London Clay
Lias Clay
Lambeth
Mercia Mudstone
Oxford Clay
Wealden
Wadhurst Clay
Carlisle
Darlington
Kendal
Blackpool
Leeds
Kingston Upon Hull
Doncaster
Manchester
Liverpool
Chesterfield
Wrexham/Wrecsam
Nottingham
Leicester
Peterborough
Newtown
Birmingham
Cambridge
Banbury
Cheltenham
Oxford
London
Reading
Bristol
Bath
Canterbury
Guildford
Dover
Taunton
Southampton
Weymouth

Figure 1

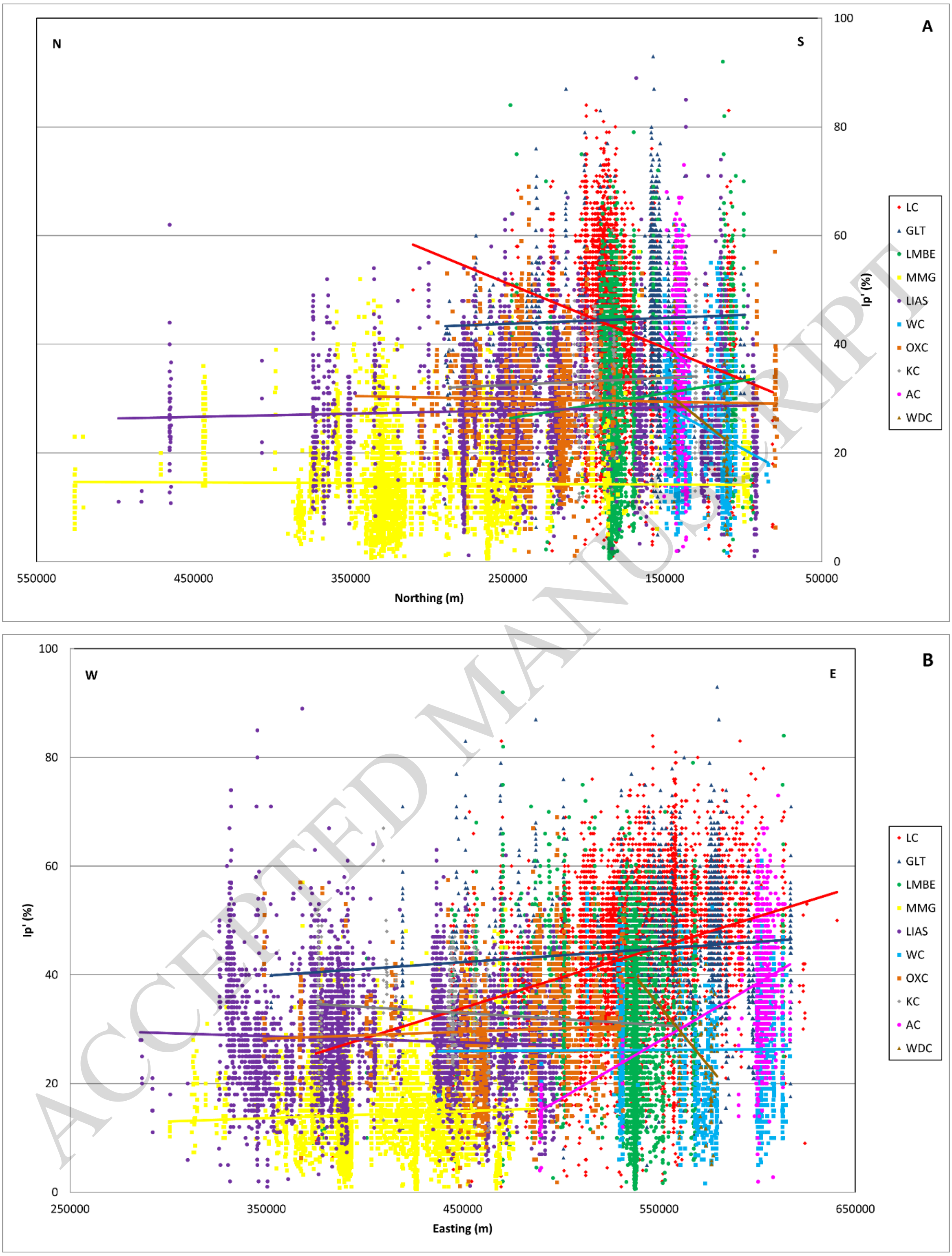
A
N
S
Ip' (%)
Northing (m)
550000
450000
350000
250000
150000
50000
0
20
40
60
80
100
LC
GLT
LMBE
MMG
LIAS
WC
OXC
KC
AC
WDC
B
W
E
Ip' (%)
Easting (m)
250000
350000
450000
550000
650000
0
20
40
60
80
100
LC
GLT
LMBE
MMG
LIAS
WC
OXC
KC
AC
WDC

Figure 2

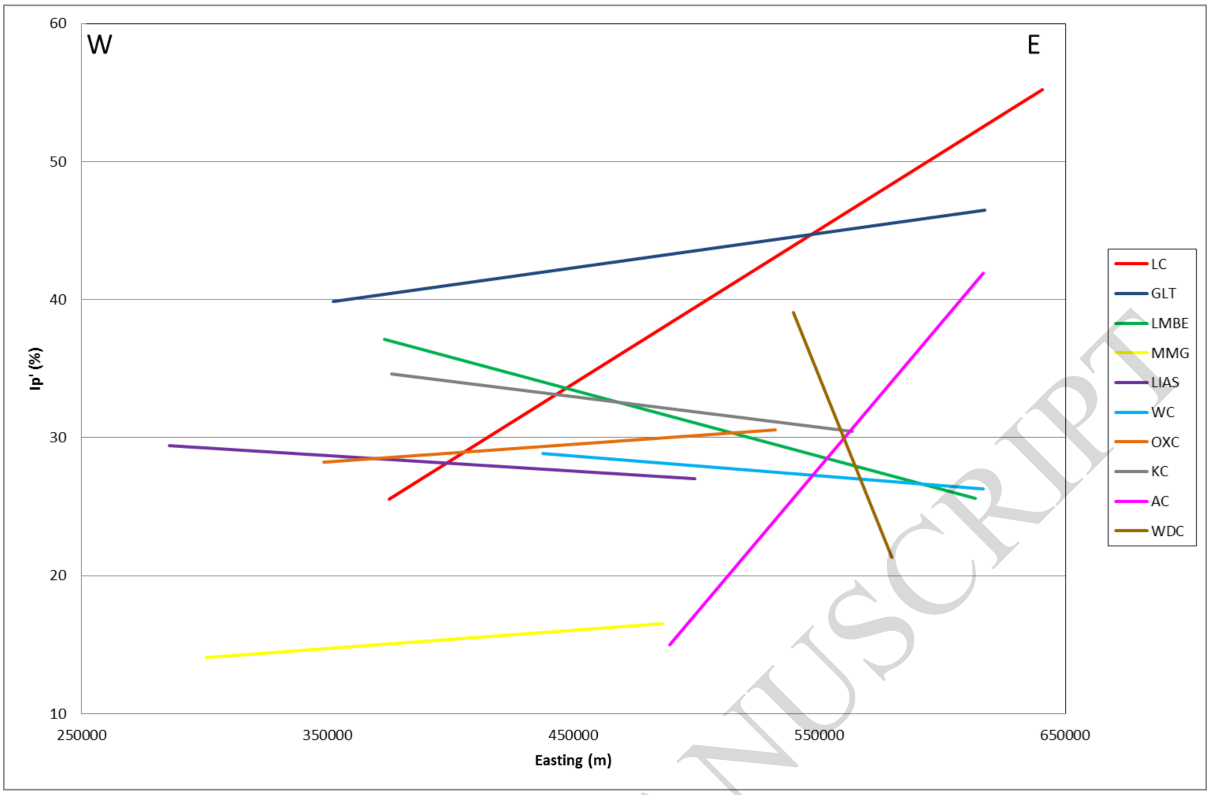
W
E
Ip' (%)
60
50
40
30
20
10
250000
350000
450000
550000
650000
Easting (m)
LC
GLT
LMBE
MMG
LIAS
WC
OXC
KC
AC
WDC

A

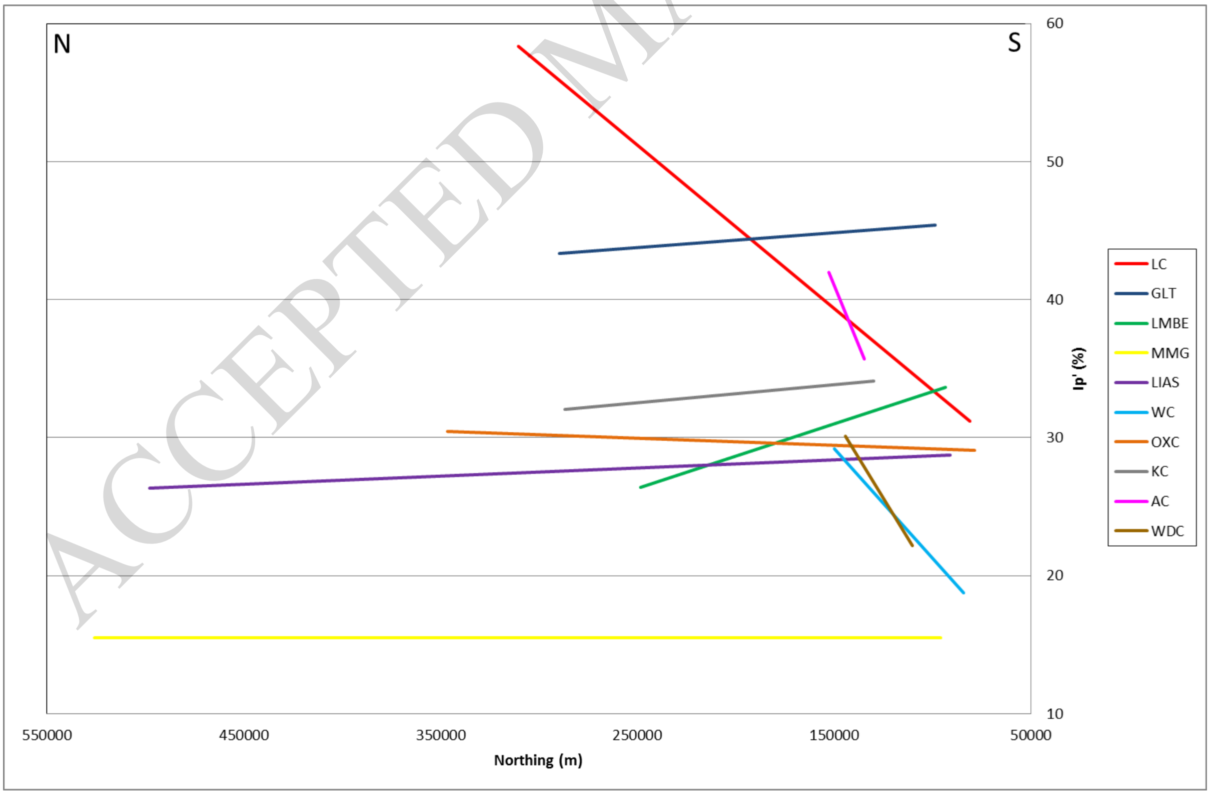
N
S
Ip' (%)
60
50
40
30
20
10
550000
450000
350000
250000
150000
50000
Northing (m)
LC
GLT
LMBE
MMG
LIAS
WC
OXC
KC
AC
WDC

B

Figure 3

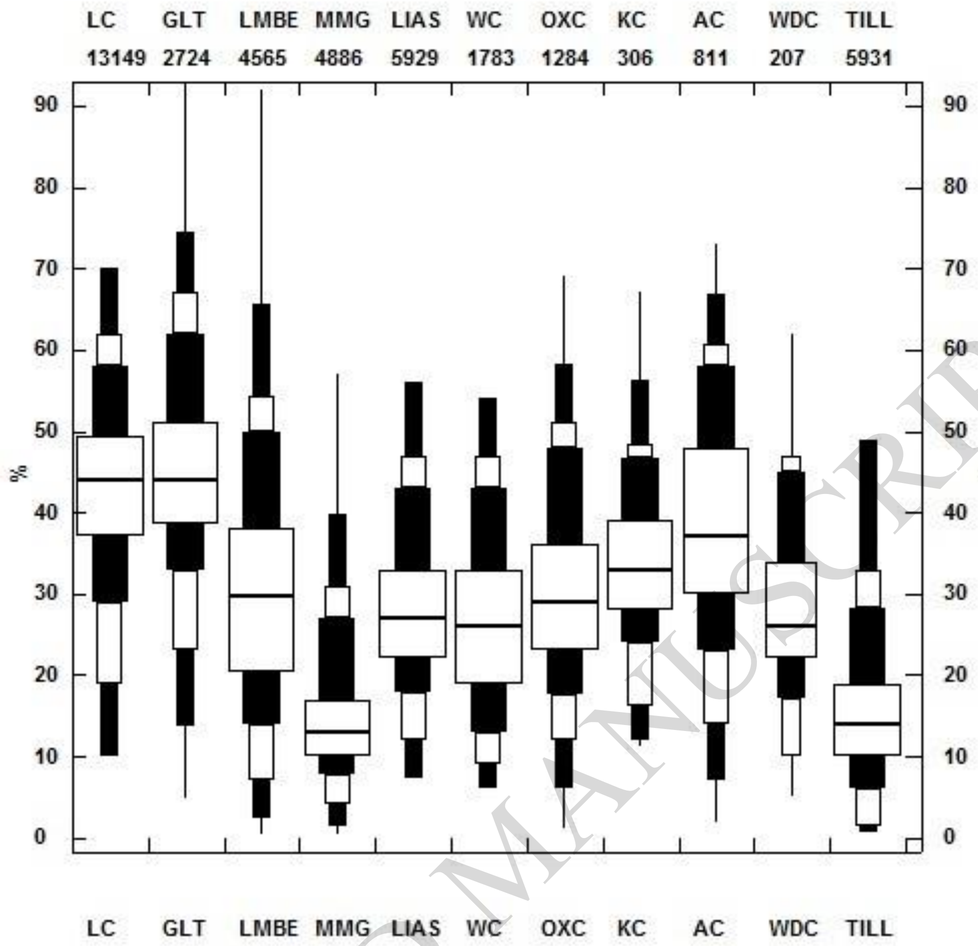
LC GLT LMBE MMG LIAS WC OXC KC AC WDC TILL
13149 2724 4565 4886 5929 1783 1284 306 811 207 5931
%
0
10
20
30
40
50
60
70
80
90
LC GLT LMBE MMG LIAS WC OXC KC AC WDC TILL

Figure 4

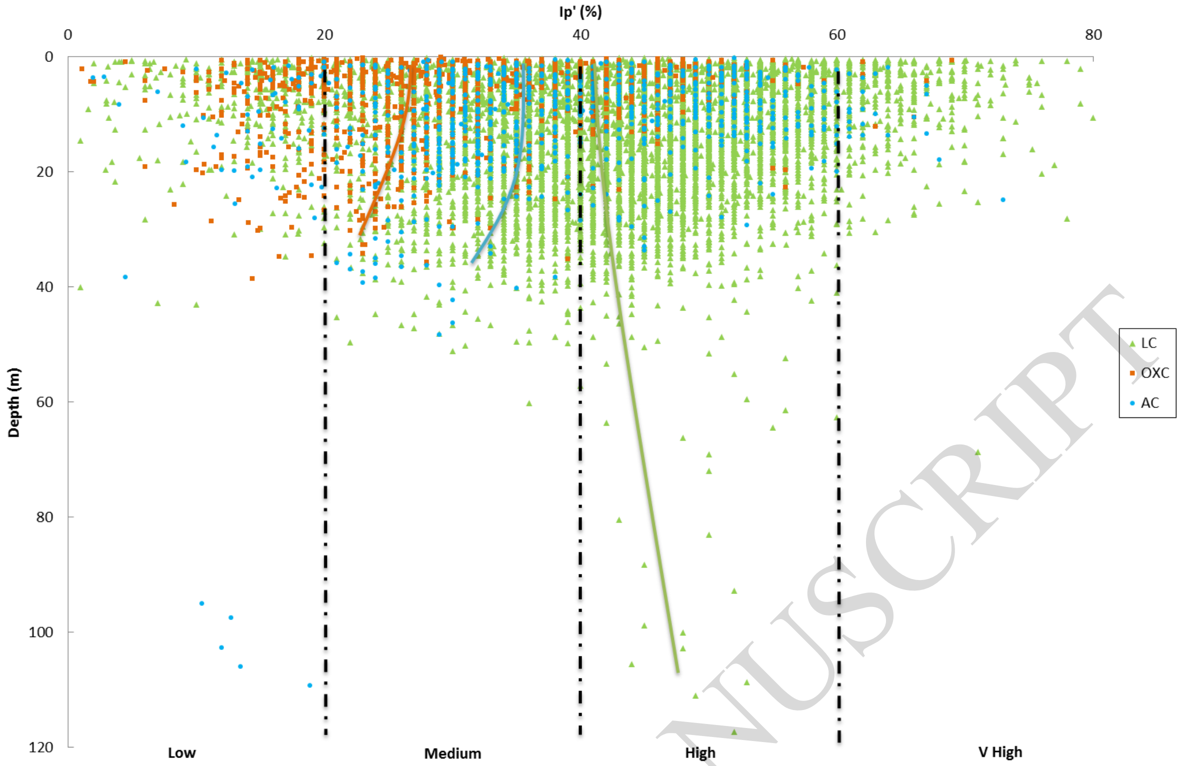


Figure 5a

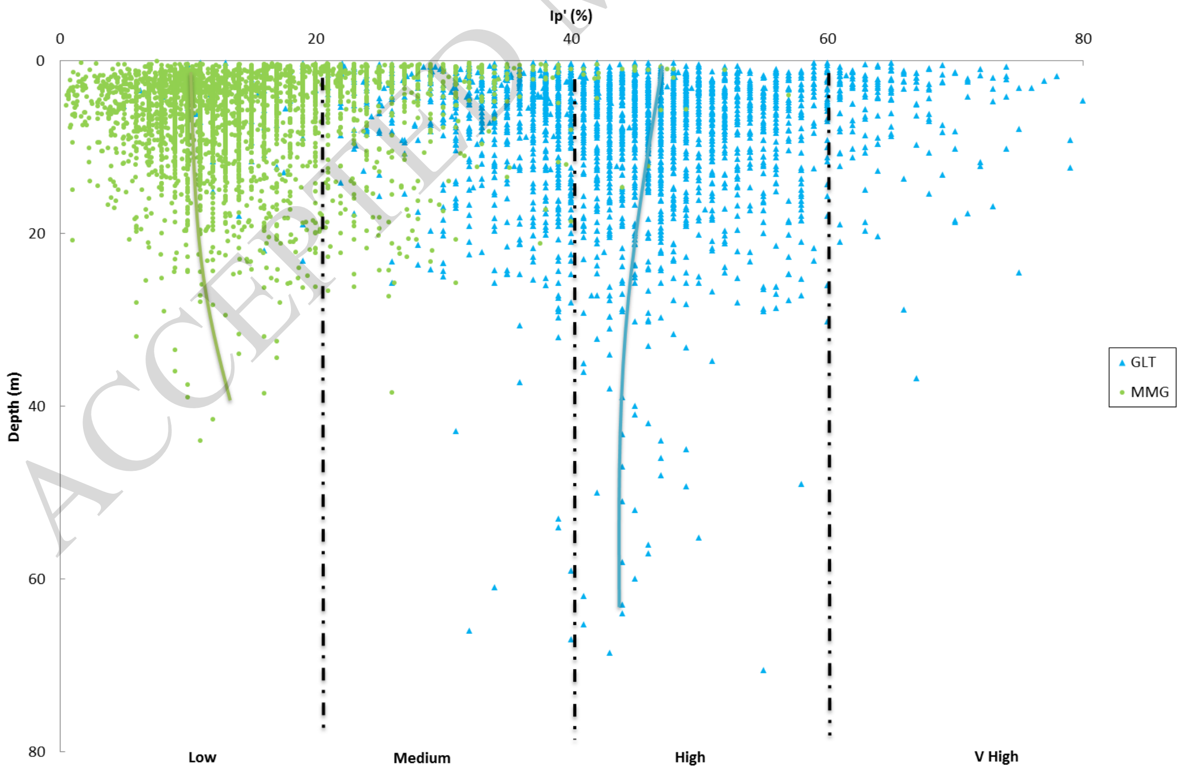


Figure 5b

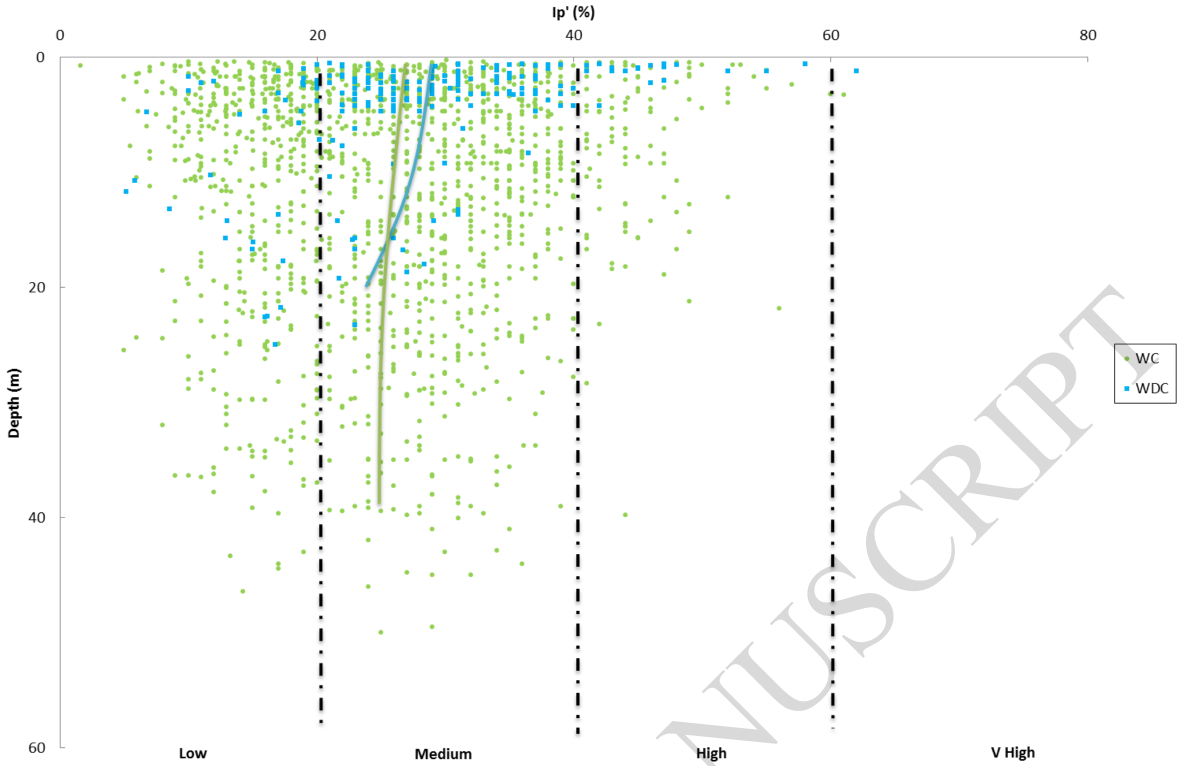


Figure 5c

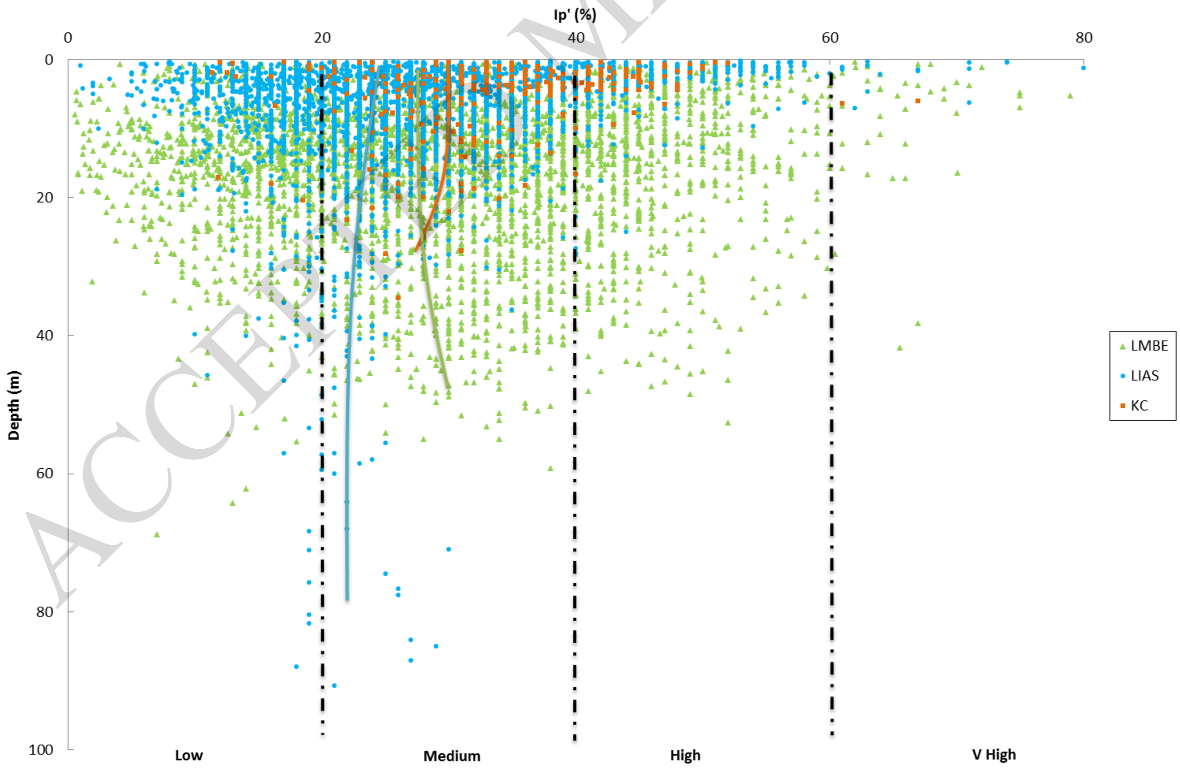


Figure 5d

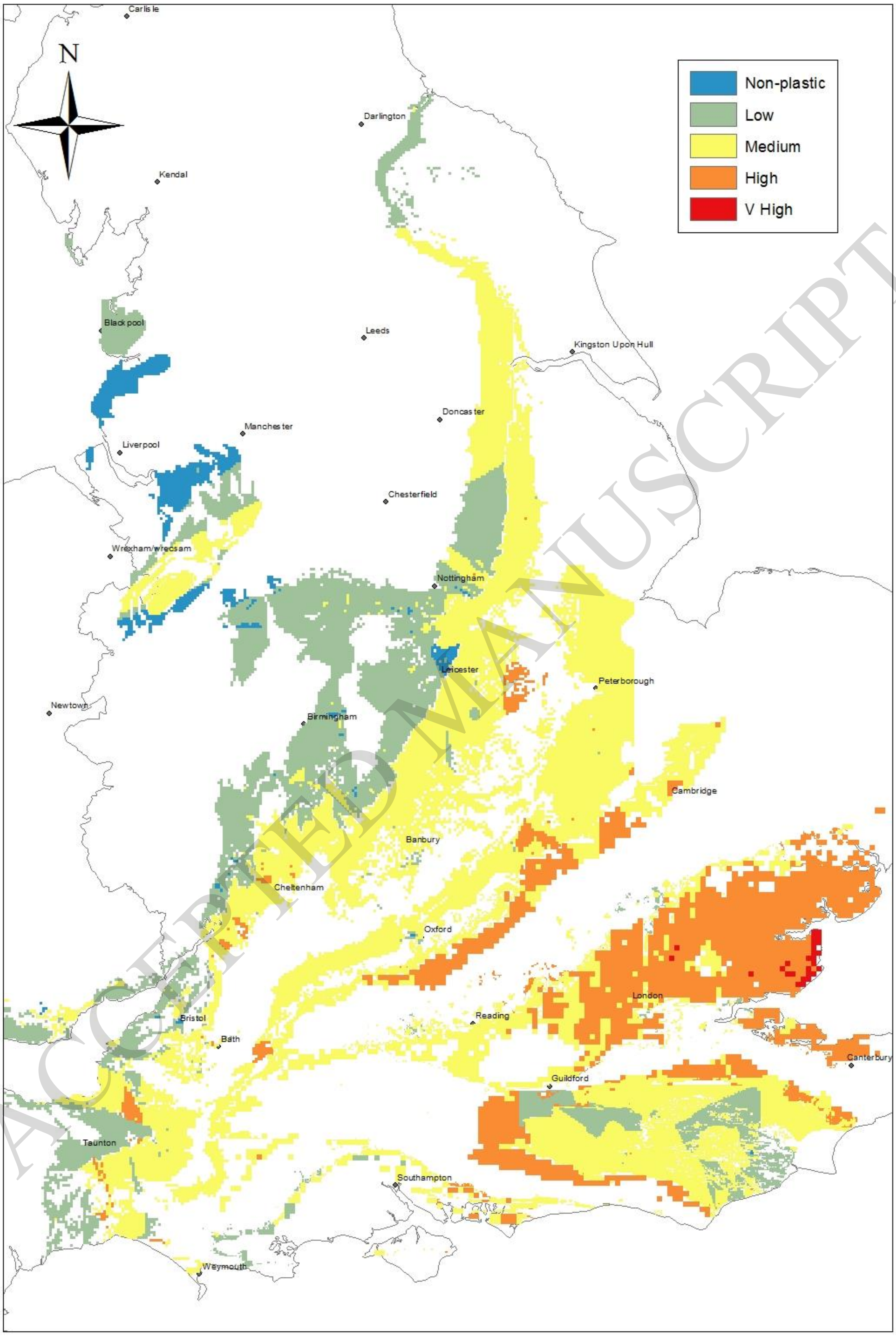
N
Non-plastic
Low
Medium
High
V High
Carlisle
Darlington
Kendal
Blackpool
Leeds
Kingston Upon Hull
Doncaster
Manchester
Liverpool
Chesterfield
Wrexham/wrecsam
Nottingham
Leicester
Peterborough
Newtown
Birmingham
Cambridge
Banbury
Cheltenham
Oxford
London
Reading
Bristol
Bath
Canterbury
Guildford
Taunton
Southampton
Weymouth



Figure 6

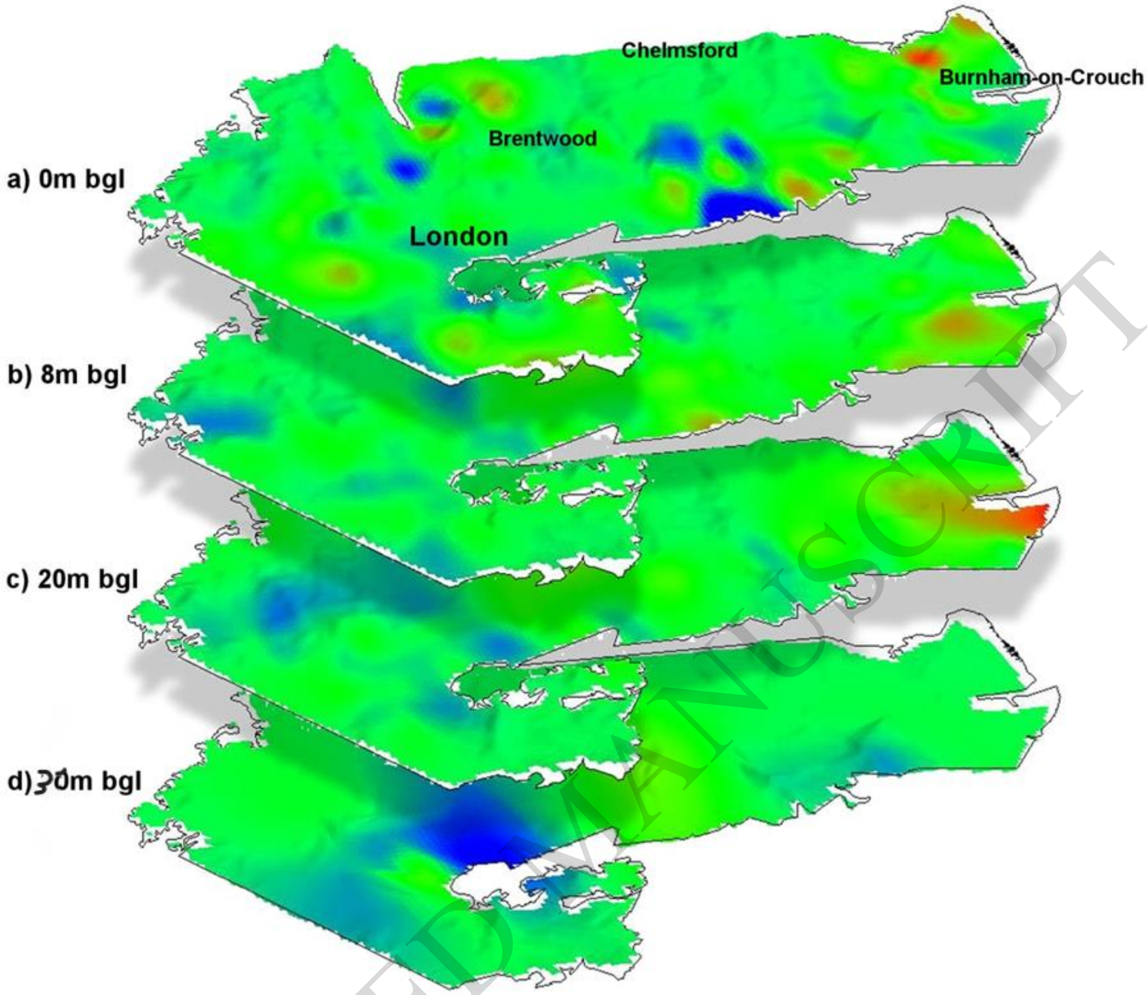
Chelmsford
Burnham-on-Crouch
Brentwood
a) 0m bgl
London
b) 8m bgl
c) 20m bgl
d) 30m bgl

Figure 7

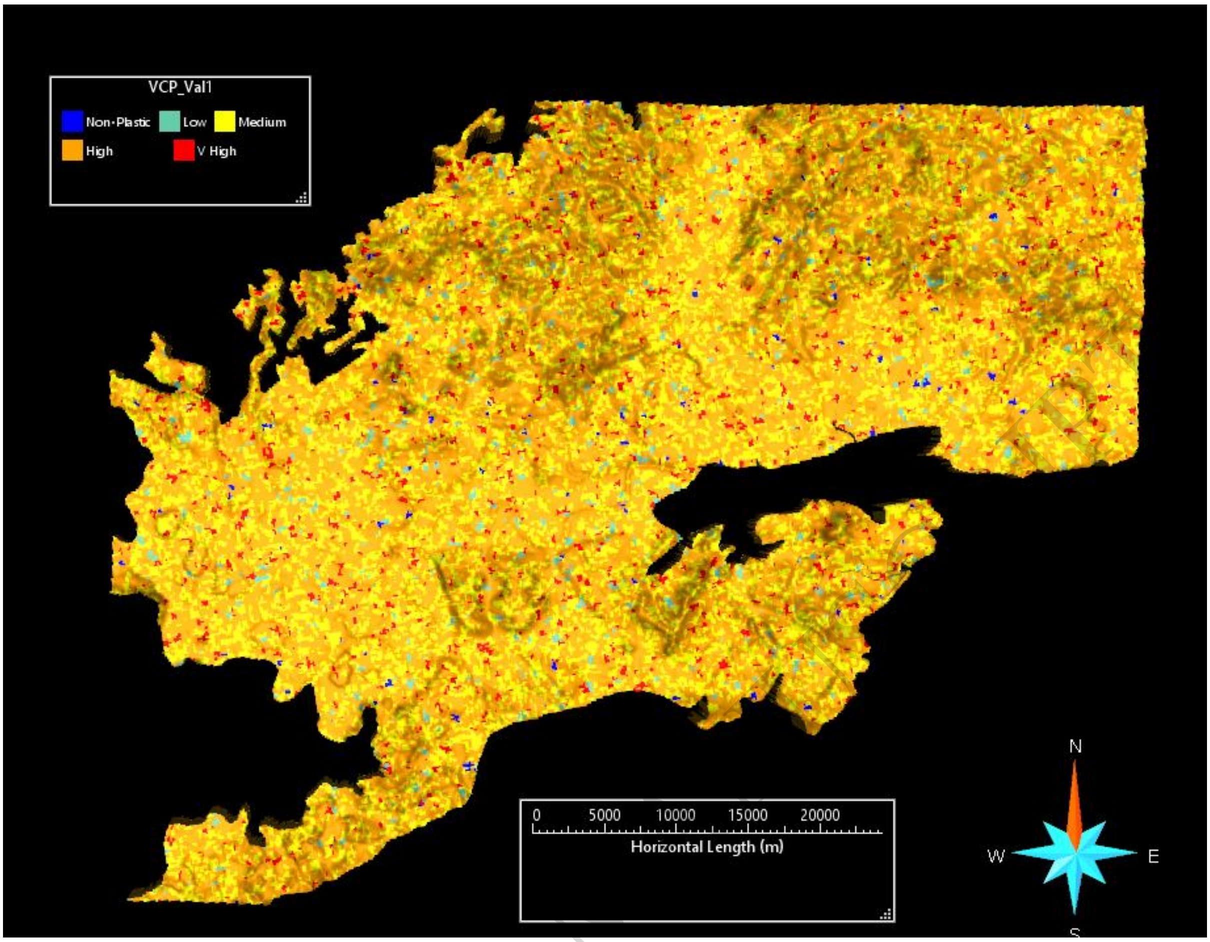
VCP_Val1
Non-Plastic
Low
Medium
High
V High
0 5000 10000 15000 20000
Horizontal Length (m)
N
W
E

Figure 8

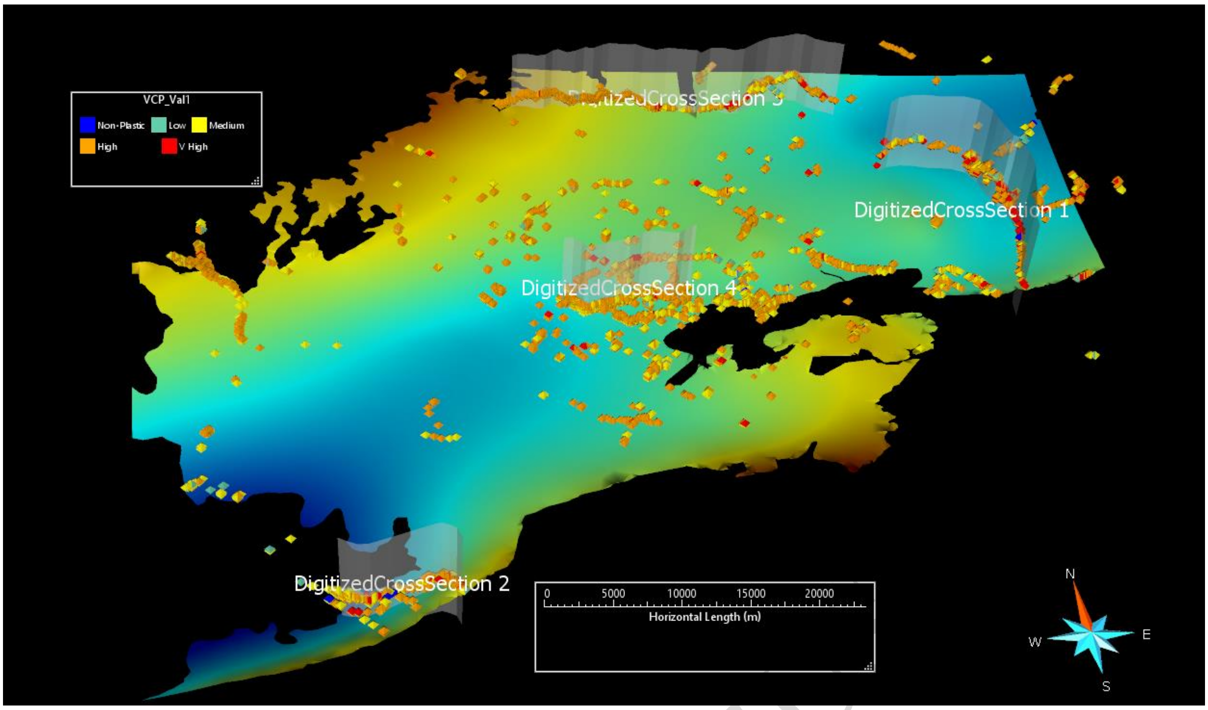
VCP_Val1
Non-Plastic
Low
Medium
High
V High
DigitizedCrossSection 1
DigitizedCrossSection 4
DigitizedCrossSection 2
0
5000
10000
15000
20000
Horizontal Length (m)
N
E
S
W

Figure 9

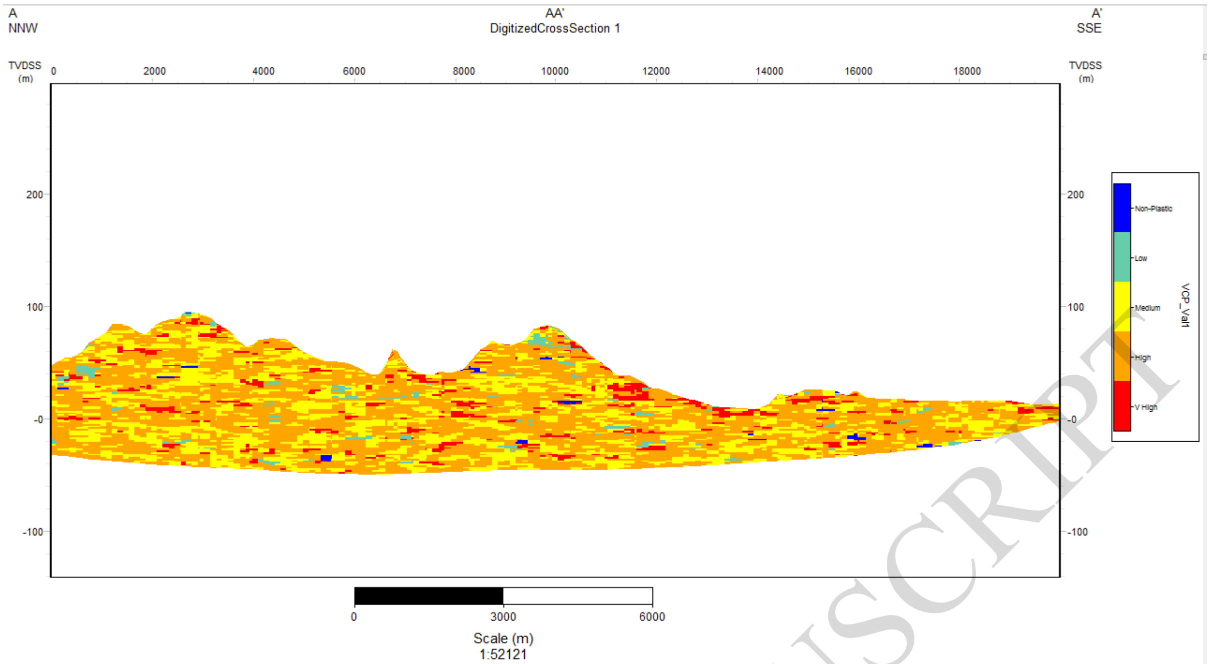

A
NNW
AA'
DigitizedCrossSection 1
A'
SSE
TVDSS (m)
0
2000
4000
6000
8000
10000
12000
14000
16000
18000
TVDSS (m)
200
100
-0
-100
Non-Plastic
Low
Medium
High
V High
VCP_Val1
0
3000
6000
Scale (m)
1:52121


Figure 10

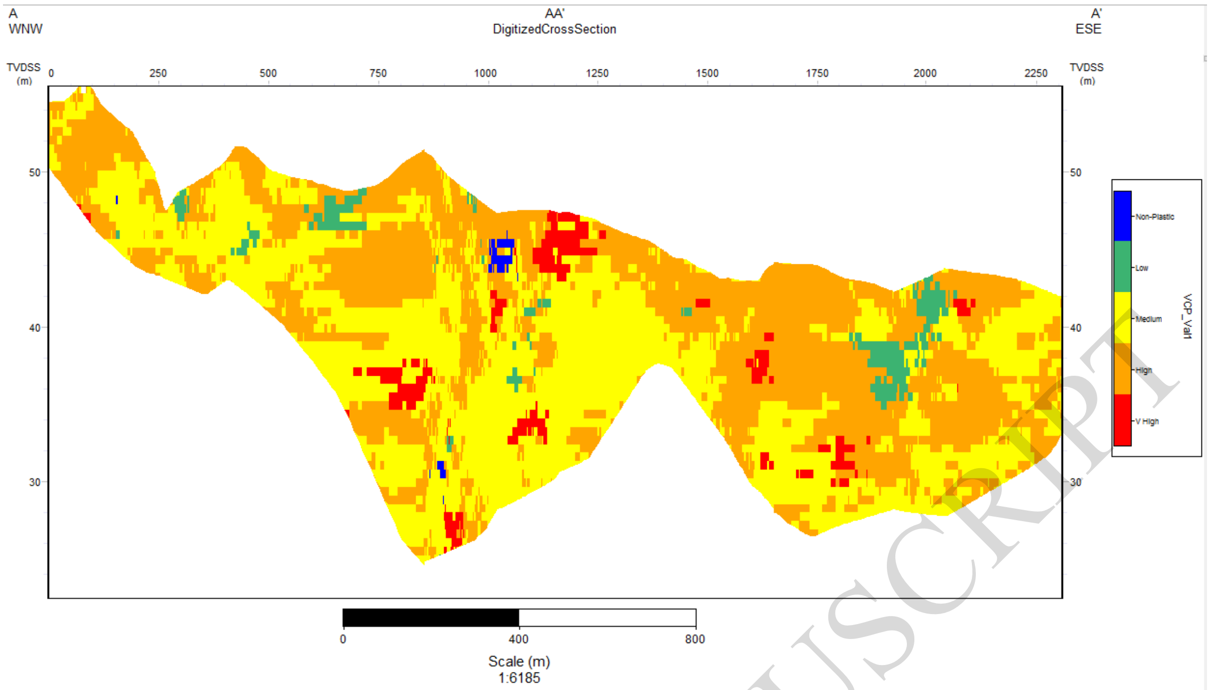
A
WNW
AA'
DigitizedCrossSection
A'
ESE
TVDSS (m)
0
250
500
750
1000
1250
1500
1750
2000
2250
50
40
30
Non-Plastic
Low
Medium
High
V High
VCP_Val1
0
400
800
Scale (m)
1:6185

Figure 11

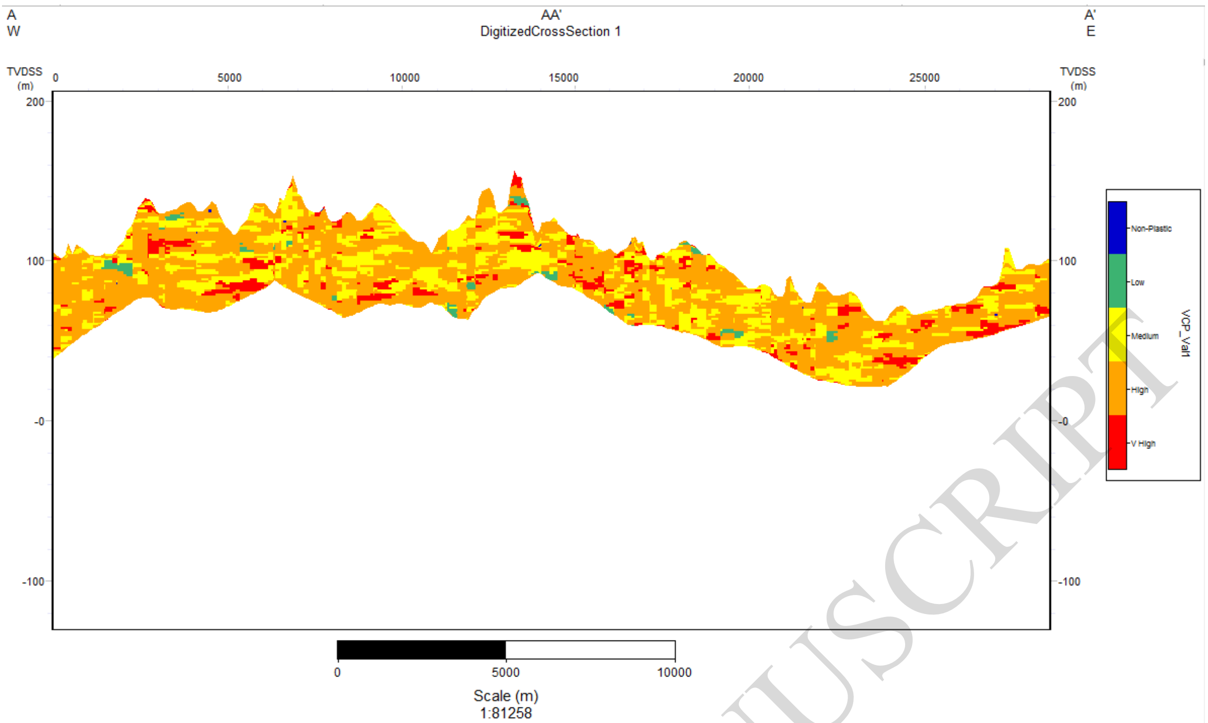
A
W
AA'
DigitizedCrossSection 1
A'
E
TVDSS (m)
0
5000
10000
15000
20000
25000
200
100
-0
-100
Non-Plastic
Low
Medium
High
V High
VCP_Val1
0
5000
10000
Scale (m)
1:81258

Figure 12

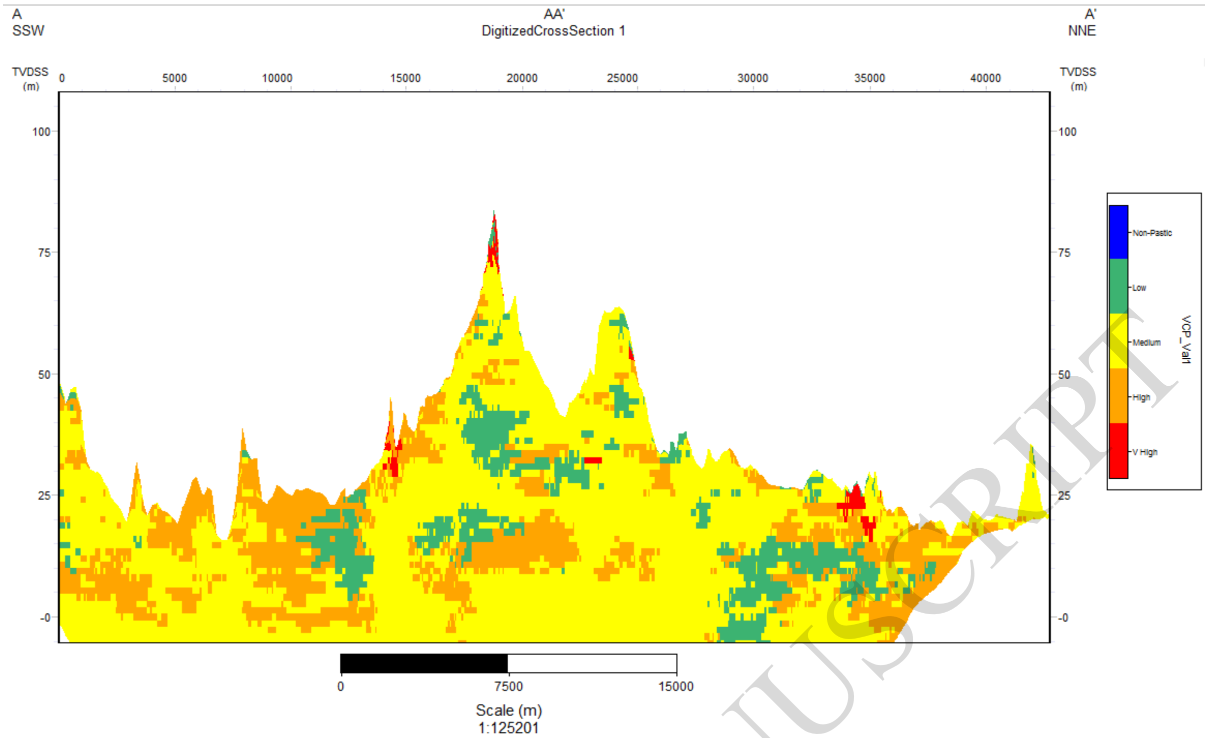
A
SSW
AA'
DigitizedCrossSection 1
A'
NNE
TVDSS
(m)
0
5000
10000
15000
20000
25000
30000
35000
40000
TVDSS
(m)
100
75
50
25
-0
Non-Pastic
Low
Medium
High
V High
VCP_Val1
0
7500
15000
Scale (m)
1:125201

Figure 13

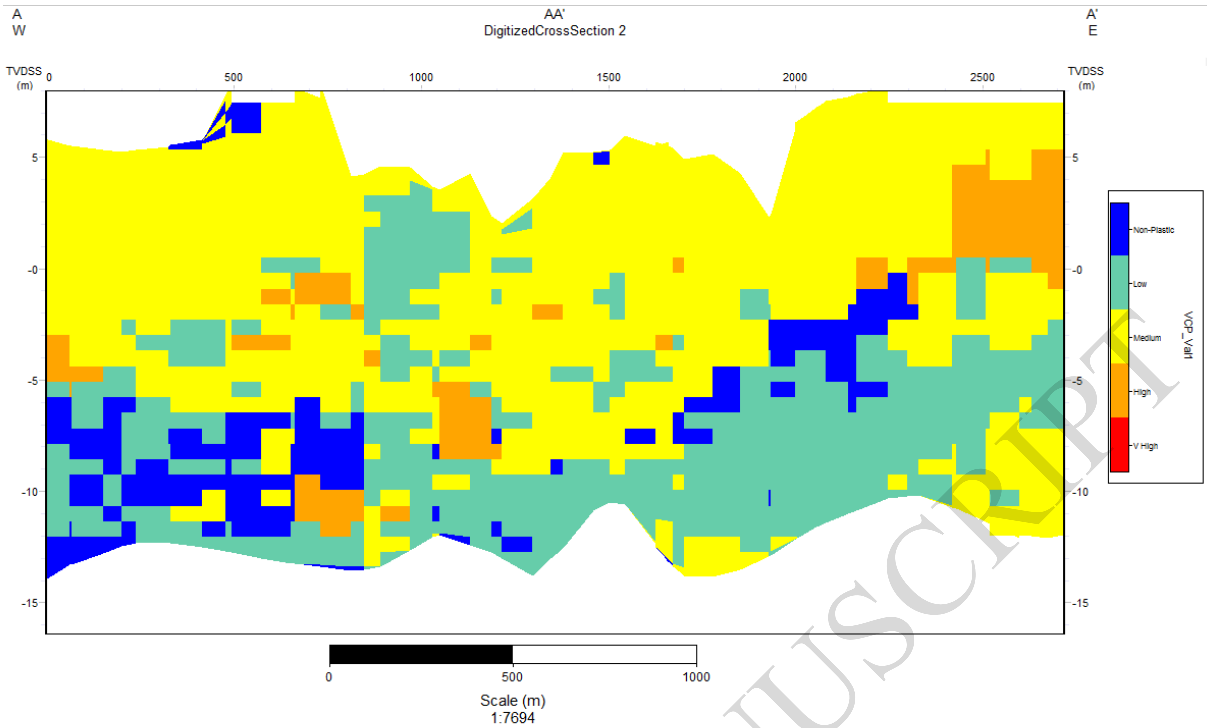
A
W
AA'
DigitizedCrossSection 2
A'
E
TVDSS
(m)
0
500
1000
1500
2000
2500
5
-0
-5
-10
-15
Non-Plastic
Low
Medium
High
V High
VCP_Val1
0
500
1000
Scale (m)
1:7694

Figure 14

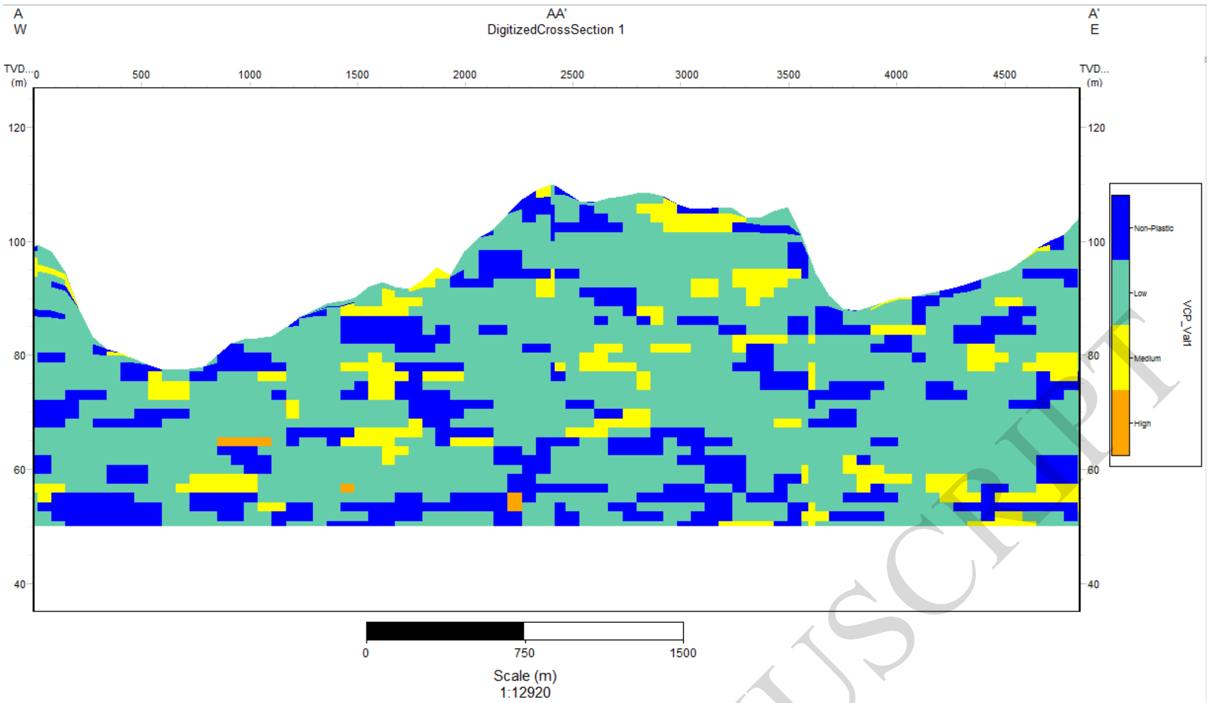
A
W
AA'
DigitizedCrossSection 1
A'
E
TVD...
(m)
0
500
1000
1500
2000
2500
3000
3500
4000
4500
120
100
80
60
40
Non-Plastic
Low
Medium
High
VCP_Val1
0
750
1500
Scale (m)
1:12920

Figure 15

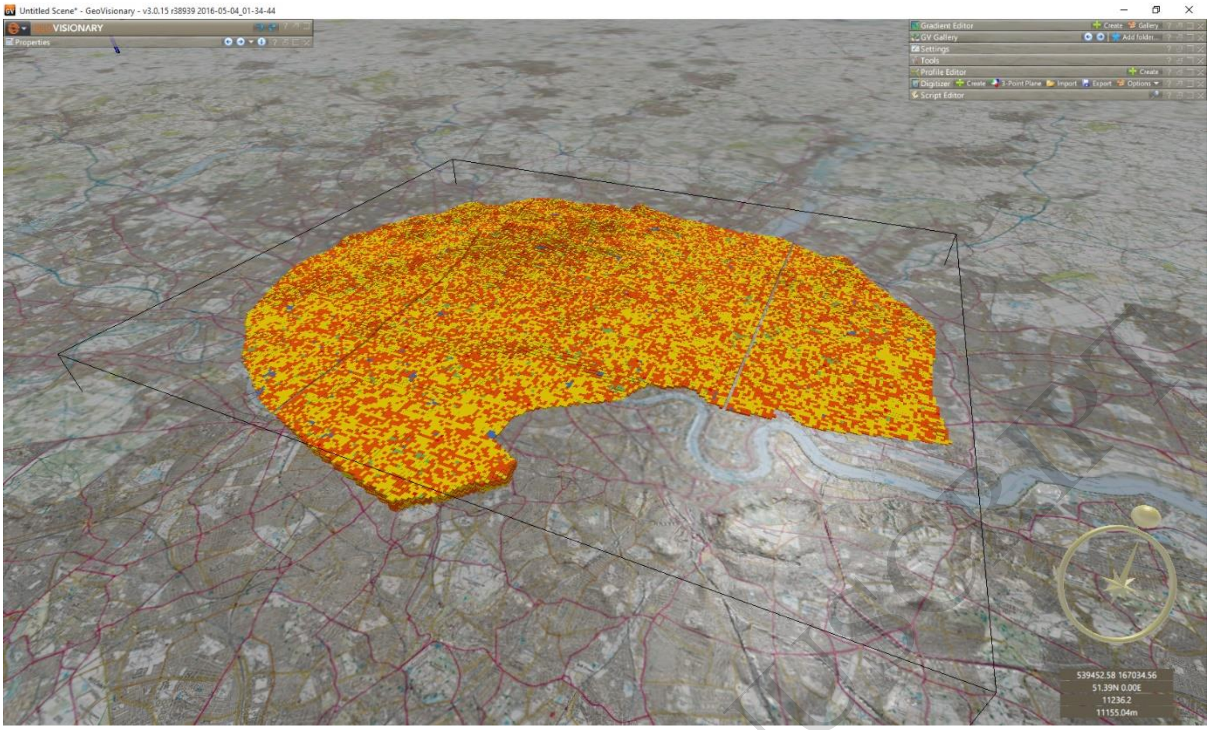
Untitled Scene* - GeoVisionary - v3.0.15 r38939 2016-05-04_01-34-44
VISIONARY
Properties
Gradient Editor
GV Gallery
Settings
Tools
Profile Editor
Digitizer
Script Editor
539452.58 167034.56
51.39N 0.00E
11236.2
11155.04m

Figure 16

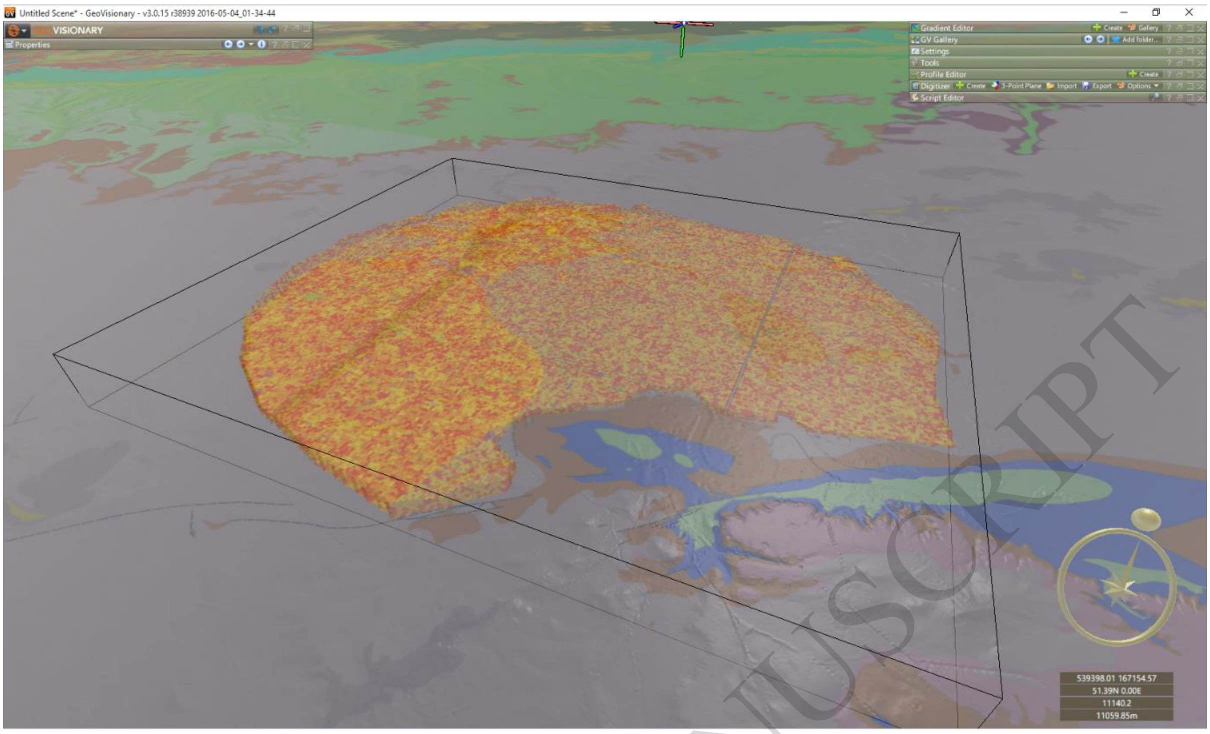
Untitled Scene* - GeoVisionary - v3.0.15 r38939 2016-05-04_01-34-44
VISIONARY
Properties
Gradient Editor
GV Gallery
Settings
Tools
Profile Editor
Digitizer
Script Editor
539398.01 167154.57
51.39N 0.00E
11140.2
11059.85m

Figure 17

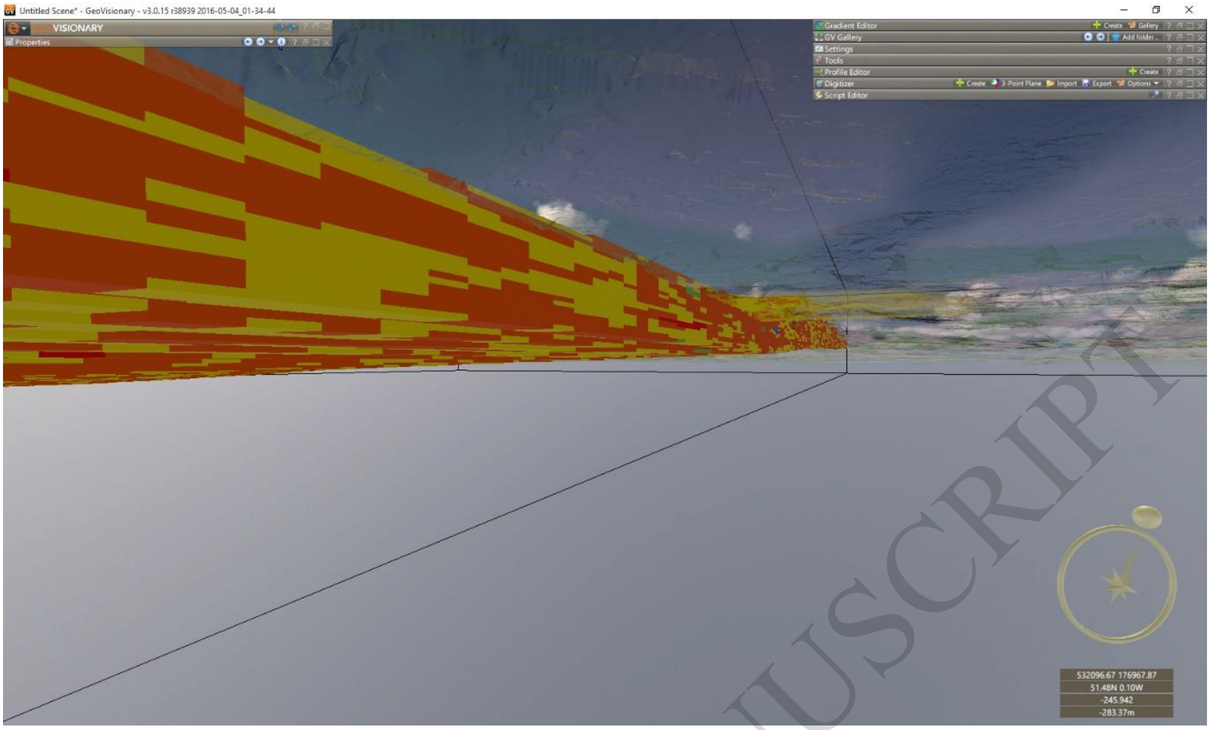
Untitled Scene* - GeoVisionary - v3.0.15 r38939 2016-05-04_01-34-44
VISIONARY
Properties
Gradient Editor
GV Gallery
Settings
Tools
Profile Editor
Digitizer
Script Editor
532096.67 176967.87
51.48N 0.10W
-245.942
-283.37m

Figure 18

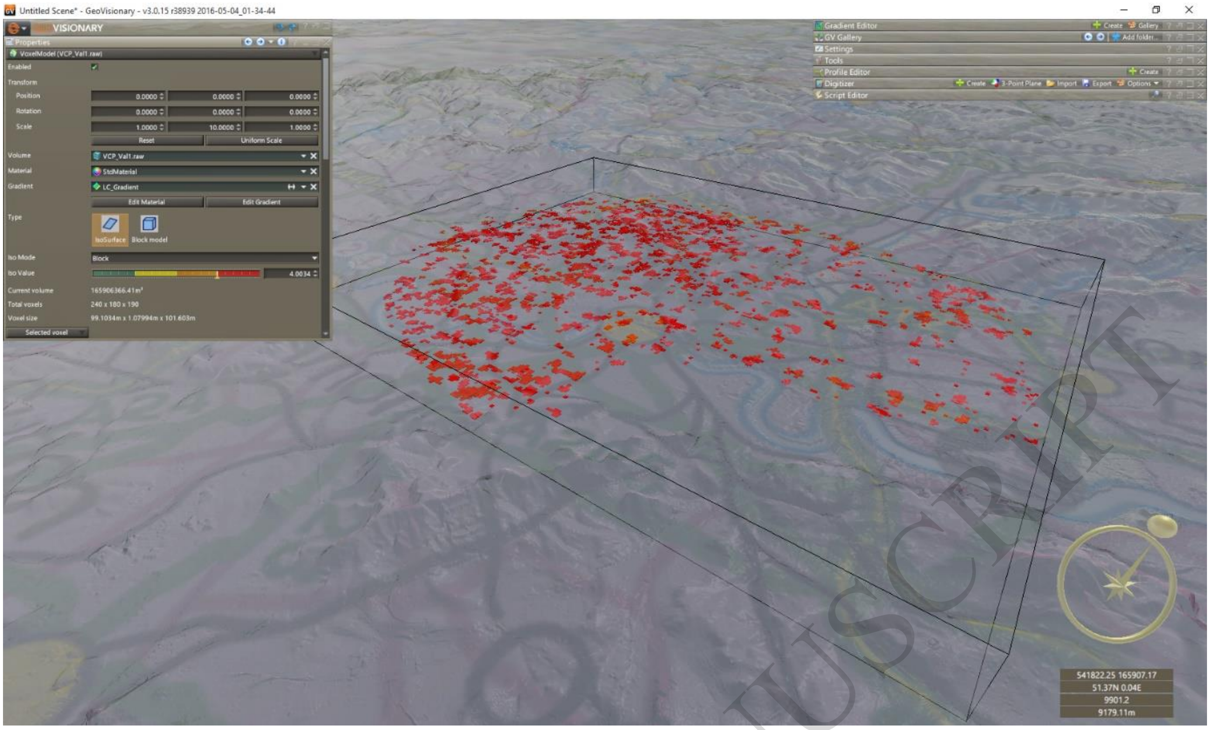

Untitled Scene* - GeoVisionary - v3.0.15 r38939 2016-05-04_01-34-44
VISIONARY
Properties
VoxelModel (VCP_Val1.raw)
Enabled
Transform
Position 0.0000 0.0000 0.0000
Rotation 0.0000 0.0000 0.0000
Scale 1.0000 10.0000 1.0000
Reset
Uniform Scale
Volume VCP_Val1.raw
Material StdMaterial
Gradient LC_Gradient
Edit Material
Edit Gradient
Type
IsoSurface
Block model
Iso Mode Block
Iso Value 4.0034
Current volume 165906366.41m³
Total voxels 240 x 180 x 190
Voxel size 99.1034m x 1.07994m x 101.603m
Selected voxel
Gradient Editor
Create
Gallery
GV Gallery
Add folder...
Settings
Tools
Profile Editor
Create
Digitizer
Create
3-Point Plane
Import
Export
Options
Script Editor
541822.25 165907.17
51.37N 0.04E
9901.2
9179.11m


Figure 19

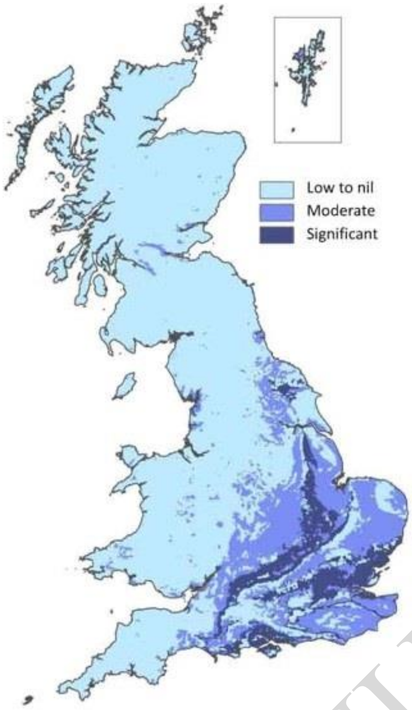


Figure 20

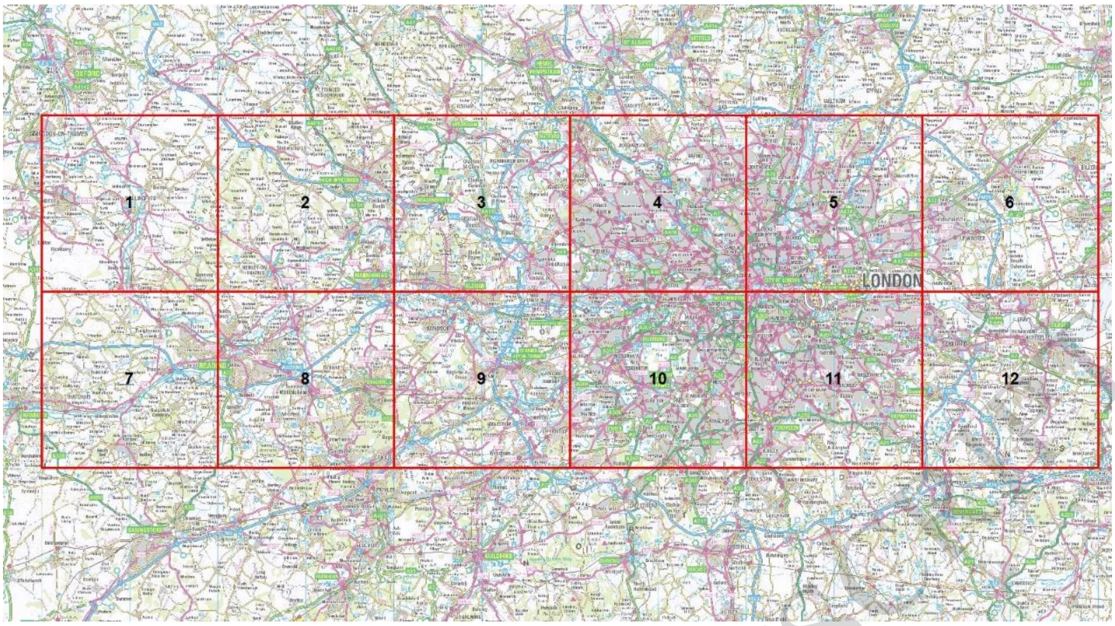


Figure 21

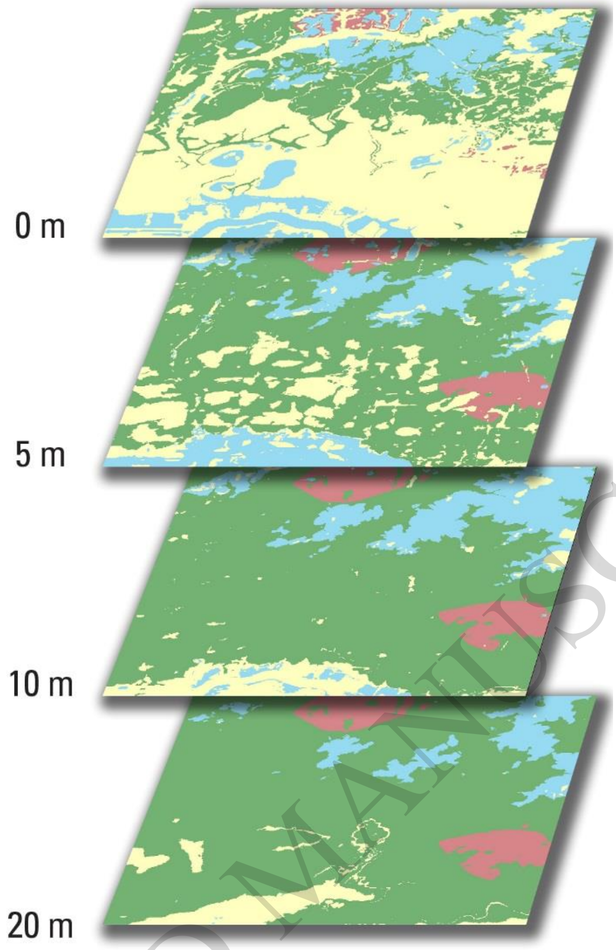


Figure 22